Sensing-Throughput Tradeoff for Interweave Cognitive Radio System: A Deployment-Centric Viewpoint

Journal:	*IEEE Transactions on Wireless Communications*
Manuscript ID:	Paper-TW-Aug-15-1167
Manuscript Type:	Original Transactions Paper
Date Submitted by the Author:	29-Aug-2015
Complete List of Authors:	Kaushik, Ankit; Karlsruhe Institute of Technology, Communications Engineering Lab Sharma, Shree Krishna; University of Luxembourg, SnT Chatzinotas, Symeon; University of Luxembourg, SnT Ottersten, Bjorn; University of Luxembourg, SnT Jondral, Friedrich; Karlsruhe Institute of Technology, Communications Engineering Lab
Keyword:	

Sensing-Throughput Tradeoff for Interweave Cognitive Radio System: A Deployment-Centric Viewpoint

Ankit Kaushik*, *Student Member, IEEE*, Shree Krishna Sharma†, *Member, IEEE*, Symeon Chatzinotas†, *Senior Member, IEEE*, Björn Ottersten†, *Fellow, IEEE*, Friedrich K. Jondral* *Senior Member, IEEE*

Abstract

Secondary access to the licensed spectrum is viable only if interference is avoided at the primary system. In this regard, different paradigms have been conceptualized in the existing literature. Of these, Interweave Systems (ISs) that employ spectrum sensing have been widely investigated. Baseline models investigated in the literature characterize the performance of IS in terms of a sensing-throughput tradeoff, however, this characterization assumes the knowledge of the involved channels at the secondary transmitter, which is unavailable in practice. Motivated by this fact, we establish a novel approach that incorporates channel estimation in the system model, and consequently investigate the impact of imperfect channel estimation on the performance of the IS. More particularly, the variation induced in the detection probability affects the detector's performance at the secondary transmitter, which may result in severe interference at the primary users. In this view, we propose to employ average and outage constraints on the detection probability, in order to capture the performance of the IS. Our analysis reveals that with an appropriate choice of the estimation time determined by the proposed model, the

*A. Kaushik and F. K. Jondral are with Communications Engineering Lab, Karlsruhe Institute of Technology (KIT), Germany. Email:{ankit.kaushik,friedrich.jondral}@kit.edu.

†S.K. Sharma, S. Chatzinotas and B. Ottersten are with SnT - securityandtrust.lu, University of Luxembourg, Luxembourg. Email:{shree.sharma, symeon.chatzinotas, bjorn.ottersten}@uni.lu.

The preliminary analysis of this paper has been presented at CROWNCOM 2015 in Doha, Qatar [1].

This work was partially supported by the National Research Fund, Luxembourg under the CORE projects "SeMIGod" and "SATSENT".

degradation in performance of the IS can be effectively controlled, and subsequently the achievable secondary throughput can be significantly enhanced.

Index Terms

Cognitive radio, Interweave system, Sensing-throughput tradeoff, Spectrum Sensing, Channel estimation

I. Introduction

We are currently in the phase of conceptualizing the requirements of the fifth generation (5G) of mobile wireless systems. One of the major goals is to improve the areal capacity (bits/s/m^2) by a factor of 1000 [2]. A large contribution of this demand is procured by means of an extension to the existing spectrum. Recently, the spectrum beyond 6 GHz, which largely entails the millimeter wave is envisaged as a powerful source of spectrum for 5G systems. However, the millimeter wave technology is still in its nascent stage and along with complex regulatory requirements in this regime, it is surmounted by key challenges like propagation loss, low efficiency of radio frequency components such as power amplifiers, small size of the antenna and link acquisition that need to be addressed [3]. Therefore, to capture a deeper insight of its feasibility in 5G, it is essential to overcome the aforementioned challenges in the forthcoming future.

In contrast, the spectrum below 6 GHz, which is appropriate especially for mobile communications, presents an alternative solution. Due to its static allocation, this spectrum is on the verge of depletion. However, it is possible to overcome this scarcity if we manage to utilize this radio spectrum efficiently. In this perspective, Cognitive Radio (CR) is foreseen as one of the potential contenders that addresses the problem of spectrum scarcity. Over the past one and a half decade, this notion has evolved at a tremendous pace right from its origin by Mitola *et al.* in 1999 [4] and consequently, it has acquired certain maturity. However, from a deployment perspective, this technology is still in its preliminary phase. In this view, it is imperative to make substantial efforts that enable the placement of this concept over a hardware platform.

An access to the licensed spectrum is an outcome to the paradigm employed by the Secondary User (SU). Based on the paradigms described in the literature, all CR systems that provide dynamic access to the spectrum fall mainly under three categories, namely, interweave, underlay and overlay systems [5]. In Interweave Systems (ISs), the SUs render an interference-free access to the licensed spectrum by exploiting spectral holes in different domains such as time, frequency, space and polarization, whereas underlay systems enable an interference-tolerant access under which the SUs are allowed to use the licensed spectrum (e.g. Ultra Wide Band) as long as they respect the interference constraints of the Primary Receivers (PRs). Besides that, overlay systems consider participation of higher layers for enabling spectral coexistence between two or more wireless networks. Due to its ease of deployment, IS is mostly preferred not only for performing theoretical analysis but for practical implementation as well. Motivated by these facts, this paper focuses on the performance analysis of the ISs from a deployment perspective.

Motivation and Related Work

Spectrum sensing is an integral part of ISs. At the Secondary Transmitter (ST), sensing is necessary for detecting the presence or absence of a primary signal, thereby protecting the PRs against harmful interference. Sensing at the ST is accomplished by listening to the signal transmitted by the Primary Transmitter (PT). For detecting a primary signal, several techniques such as energy, matched filtering, cyclostationary and feature-based detection exist [6], [7]. Because of its versatility towards unknown primary signals and its low computational complexity, energy detection has been extensively investigated in the literature [8]–[12]. In energy detection, the decision is accomplished by comparing the power received at the ST to a threshold. In reality, the ST encounters variation in the received power due to existence of thermal noise at the receiver and channel fading. This leads to sensing errors described as misdetection or false alarm, thus, limiting the performance of the IS. In order to determine the performance of the detector, it is essential to characterize the expressions of detection probability and false alarm probability.

In particular, detection probability is critical for the primary system because it protects the PR from the interference induced by the ST. As a result, sustaining a target detection probability is of paramount importance to the ISs [13]. Therefore, the characterization of the detection probability becomes absolutely necessary for the performance analysis of the IS. In this context, Urkowitz [8] introduced a probabilistic model that establishes a fundamental framework for characterizing the sensing errors, however, the characterization accounts only for noise in the system. To encounter the variation caused by channel fading, a frame structure is introduced such that the channel is considered to remain constant over the frame duration, however, upon exceeding the frame duration, the system may witness a different realization of the channel. Based on this frame structure, the performance of the IS has been investigated as *short-term* [14]–[16] and *long-term* [9]–[11] characterization.

The long-term (statistical) characterization is a classical approach that applies a fading model to average out the variation in the received power. Subject to the deployment scenarios[1], different fading models – Rice, Rayleigh, Nakagami-m and Log-normal can be employed [17]. The analytical expressions for the expected detection probability for these fading models are characterized in [9]–[11]. Considering a CR system, this approach has some major drawbacks. Fading models depict a long-term characterization of the system, however, short-term or bursty interference that may lead to outage is ignored, thereby deteriorating the performance of a primary system. Moreover, fading models are specific to the deployment scenario, hence, knowledge of the fading model is necessary when designing a CR system. Apart from that, every fading model contains certain model parameters. As a result, estimation of these parameters at the ST [18], particularly during the initial phase of the deployment, imposes an additional overhead on the secondary system. In practice, due to mobility, most systems are likely to violate stationarity over a long duration. Thus, it becomes challenging to track these model parameters. As a consequence, these drawbacks restrict the applicability of this approach to practical CR systems.

To overcome the aforementioned drawbacks, an alternative approach that considers the short-term characterization has been established [14]–[16] in such a way that the performance can be analyzed for a single frame[2]. In this way, unlike long-term approach, we preclude the variation due to the channel and consider the variation due to noise in the system. Subsequently, this approach does not need to consider the deployment of the fading model and its complexities thereafter. Motivated by these facts, we focus on the short-term approach for performance analysis.

[1]These scenarios include urban, suburban and rural, or indoor and outdoor from a different perspective.

[2]By a single frame, we refer to the statistical realizations of the received power, whereas [14]–[16] consider the temporal realizations of the same across several frames. Considering ergodic behaviour of the noise, the performance characterization under these two scenarios are equivalent.

Problem Formulation

Recently, the performance characterization of CR systems in terms of sensing-throughput tradeoff has received significant attention [14], [16], [19], [20]. According to Liang *et al.* [14], the ST assures a reliable detection of a primary signal, thereby sustaining the detection probability above a desired level with an objective of maximizing the throughput at the Secondary Receiver (SR). In this way, the sensing-throughput tradeoff renders a suitable sensing time that achieves a maximum throughput for a given received power. However, to characterize the detection probability and throughput, the system requires the knowledge of interacting channels, namely, a *sensing* channel, an *access* channel and an *interference* channel, cf. Fig. 1[3]. To the best of the authors' knowledge, the baseline models investigated in the literature assume the knowledge of these channels to be available at the ST. However, in practice, this knowledge is not available, thus, needs to be estimated at the ST. As a result, the existing solutions for the IS are considered idealistic for performing analysis, however, they are not suitable for deployment.

Following the previous discussion, it is apparent that the received power, contained in the sensing channel, is crucial for characterizing the detection probability, therefore, is essential for evaluating the detector's performance. The channel, according to the short-term characterization, is regarded as unknown and expected to remain constant over a frame duration, hence, it is reasonable to include received power based estimation for each frame [1]. Inherent to the estimation process, a variation is induced in the detection probability. In this sense, characterizing the performance of a detector with received power estimation remains an open problem. Besides detection probability, false alarm probability largely affects the throughput attained by the secondary system at the SR. Further, the characterization of the false alarm probability requires the knowledge of the noise power. Subject to a given uncertainty [21], this knowledge can be acquired through hardware calibration. In parallel to that, the variation in the detection probability further translates to the variation in the secondary system's throughput. Moreover, the estimation of the access and the interference channels imposes an additional variation on the throughput. Hence, to characterize the performance of the IS in terms of sensing-throughput tradeoff, it is essential to capture these variations in an accurate manner.

[3]As the interference to the PR is controlled by a regulatory constraint over the detection probability, in this view, the interaction with the PR is excluded in the considered scenario [14].

In order to overcome these difficulties, the following strategy is pursued in this paper. Firstly, we consider received power estimation at the ST that allows us to constrain the detection probability at a desired level. However, with the inclusion of this estimation, the system anticipates: (i) a performance loss in terms of temporal resources used and (ii) variations in the aforementioned performance parameters due to imperfect estimation. A preliminary analysis of this performance loss was carried out in [1], where it was revealed that in low signal to noise ratio regime, imperfect estimation of received power corresponds to large variation in detection probability, hence, causing a severe degradation in the performance of the IS. However, this performance degradation was determined by means of lower and upper bounds. In this work, we consider a more exact analysis, whereby we capture the variation in detection probability by characterizing its distribution function. Using this, we apply new probabilistic constraints on the detection probability that allow IS to operate at low signal to noise ratio regime.

Besides that, we include channel estimation at the SR to acquire the knowledge of the access and interference channels. It is well-known that systems with transmitter information (which includes the filter, pilot symbols, modulation type and time-frequency synchronization) at the receiver acquire channel knowledge by listening to the pilot data sent by the ST [22]–[25]. Other systems, where the receiver possesses either no access to this information or limited by hardware complexity, procure channel knowledge indirectly by estimating a different parameter, for instance, received signal strength or received power, that entails the channel knowledge. Recently, pilot based estimation [26], [27] and received power estimation [28] have been applied to obtain channel knowledge for CR systems. However, the analysis was restricted to underlay systems, where the emphasis was laid on modelling the interference at the PR. In this paper, we extend this concept to the IS, hence, employ pilot based estimation for the access channel and received power based estimation for the sensing and interference channels, cf. Fig. 1. Upon acquiring the knowledge of these channels at the ST, we depict the impact of imperfect channel estimation on the performance of the IS in terms of sensing-throughput tradeoff. Unlike the sensing channel, the access and interference channels have to be estimated at the SR and made available at the ST over a low-rate feedback channel.

Contributions

The major contributions of this paper can be summarized as follows:

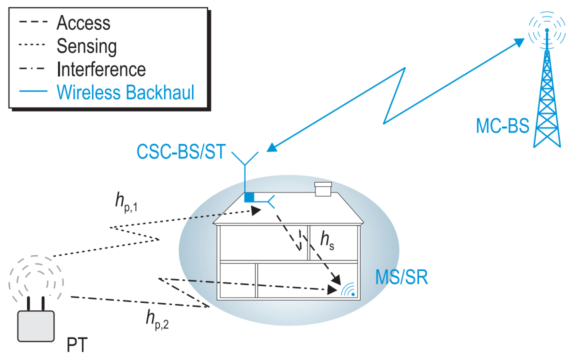

Fig. 1. A cognitive small cell scenario demonstrating: (i) the interweave paradigm, (ii) the associated network elements, which constitute Cognitive Small Cell-Base Station/Secondary Transmitter (CSC-BS/ST), Mobile Station/Secondary Receiver (MS/SR), Macro Cell-Base Station (MC-BS) and Primary Transmitter (PT), (iii) the interacting channels: sensing, access and interference.

- The main goal of the paper is to establish a system model that constitutes the estimation of: (i) sensing channel at the ST, (ii) access and (iii) interference channels at the SR. With the inclusion of estimation, the system witnesses variations in the performance parameters and a certain performance loss. Based on the proposed model, this work investigates these two aspects and characterizes the performance of the IS under realistic conditions.
- To capture the variations induced in the system, we characterize the distribution of performance parameters such as detection probability and achievable secondary throughput. More importantly, we utilize the distribution of the detection probability to establish new Primary User (PU) constraints on the detection probability.
- Subject to the new constraints, we establish the expressions of sensing-throughput tradeoff to capture the variations in the performance parameters and evaluate the performance loss in terms of the achievable throughput of the IS.
- Finally, we depict a fundamental tradeoff between estimation time, sensing time and achievable secondary throughput. We exploit this tradeoff to determine a suitable estimation and sensing time that depicts the maximum achievable performance of the IS.

Organization

The subsequent sections of the paper are organized as follows: Section II describes the system model that includes the deployment scenario, the signal model and the performance characterization for the ideal scenario for the IS. Section III presents the proposed model that incorporates channel estimation. Section IV characterizes the distribution of the performance parameters and establishes the sensing-throughput tradeoff subject to average and outage constraints. Section V analyzes the numerical results based on the obtained expressions. Finally, Section VI concludes the paper. Table I lists the definitions of acronyms and important mathematical notations used throughput the paper.

II. System Model

Deployment Scenario

Cognitive Small Cell (CSC), a CR application, characterizes a small cell deployment that fulfills the spectral requirements for Mobile Stations (MSs) operating indoor, cf. Fig. 1. For the disposition of the CSC in the network, the following key elements are essential: a CSC-Base Station (CSC-BS), a Macro Cell-Base Station (MC-BS) and MS, cf. Fig. 1. MSs are the indoor devices served by the CSC-BS over an access channel (h_{s}). Furthermore, the MC-BS is connected to several CSC-BSs over a wireless backhaul[4]. Moreover, the transmissions from the PT can be listened by the CSC-BS and the MS over sensing ($h_{\text{p,1}}$) and interference channel ($h_{\text{p,2}}$), respectively. Considering the fact that the IS is employed at the CSC-BS, the CSC-BS and the MS represent ST and SR, respectively. A hardware prototype of the CSC-BS operating as IS was presented in [29]. For simplification, a PU constraint based on false alarm probability was considered in [29]. With the purpose of improving system's reliability, we extend the analysis to employ a PU constraint on the detection probability.

As a follow-on from the ideal model depicted in [14], we consider a slotted medium access for the IS, where the time axis is segmented into frames of length T, according to which, the ST employs periodic sensing. Hence, each frame consists of a sensing slot τ_{sen} and the remaining duration $T - \tau_{\text{sen}}$ is utilized for data transmission. For small T relative to the PU's expected ON/OFF period, the requirement of the ST to be in alignment to PUs' medium access can be relaxed [30]–[32].

[4]A wireless backhaul is a point-to-point wireless link between the CSC-BS and MC-BS that relays the traffic generated from the CSC to the core network.

TABLE I

DEFINITIONS OF ACRONYMS AND NOTATIONS USED

Acronyms and Notations	**Definitions**
AC, OC	Average Constraint, Outage Constraint
CR	Cognitive Radio
CSC, CSC-BS, MC-BS, MS	Cognitive Small Cell, Cognitive Small Cell-Base Station, Macro Cell-Base Station, Mobile Station
IM, EM	Ideal Model, Estimation Model
IS	Interweave System
PU - PT, PR	Primary User - Primary Transmitter, Primary Receiver
SU - ST, SR	Secondary User - Secondary Transmitter, Secondary Receiver
$\mathcal{H}_1, \mathcal{H}_0$	Signal plus noise hypothesis, noise only hypothesis
f_s	Sampling frequency
$\tau_\mathrm{est}, \tau_\mathrm{sen}$	Estimation time, sensing time interval
T	Frame duration
$\mathrm{P_d}, \mathrm{P_{fa}}$	Probability of detection, false alarm probability
$\bar{\mathrm{P}}_\mathrm{d}$	Target detection probability
κ	Outage Constraint over detection probability
$h_\mathrm{p,1}, h_\mathrm{p,2}, h_\mathrm{s}$	Channel coefficient for the link PT-ST, PT-SR, ST-SR
$\gamma_\mathrm{p,1}, \gamma_\mathrm{p,2}, \gamma_\mathrm{s}$	Signal to noise ratio for the link PT-ST, PT-SR, ST-SR
R_s	Throughput at SR
$\mathrm{C}_0, \mathrm{C}_1$	Shanon capacity at SR without and with interference from PT
μ	Threshold for the energy detector
$F_{(\cdot)}$	Cumulative distribution function of random variable $(\cdot)$
$f_{(\cdot)}$	Probability density function of random variable $(\cdot)$
$\hat{(\cdot)}$	Estimated value of $(\cdot)$
$\tilde{(\cdot)}$	Suitable value of the parameter $(\cdot)$ that achieves maximum performance
$\mathbb{E}_{(\cdot)}$	Expectation with respect to $(\cdot)$
$\mathbb{P}$	Probability measure
$\mathbf{T}(\cdot)$	Test statistics
σ_x^2, σ_w^2	Signal variance at PT, noise variance at ST and SR
N_s	Number of pilot symbols used for pilot based estimation at the SR for h_s
$N_\mathrm{p,2}$	Number of samples used for received power estimation at the SR for $h_\mathrm{p,2}$

Signal model

Subject to the underlying hypothesis that illustrates the presence $(\mathcal{H}_1)$ or absence $(\mathcal{H}_0)$ of a primary signal, the discrete and real signal received at the ST is given by

$$y_{\mathrm{ST}}[n] = \begin{cases} h_{\mathrm{p},1} \cdot x_{\mathrm{PT}}[n] + w[n] & : \mathcal{H}_1 \\ w[n] & : \mathcal{H}_0 \end{cases}, \tag{1}$$

where $x_{\mathrm{PT}}[n]$ corresponds to a discrete and real sample transmitted by the PT, $|h_{\mathrm{p},1}|^2$ represents the power gain of the sensing channel for a given frame and $w[n]$ is additive white Gaussian noise at the ST. In [14], the primary signal $x_{\mathrm{PT}}[n]$ has been modelled as: (i) phase shift keying modulated signal, or (ii) Gaussian signal. The signals that are prone to high inter-symbol interference or entail precoding can be modelled as Gaussian signals. For this paper, we focus our analysis on the latter case. As a result, mean and variance for the signal and the noise are determined as $\mathbb{E}\left[x_{\mathrm{PT}}[n]\right] = 0$, $\mathbb{E}\left[w[n]\right] = 0$, $\mathbb{E}\left[|x_{\mathrm{PT}}[n]|^2\right] = \sigma_x^2$ and $\mathbb{E}\left[|w[n]|^2\right] = \sigma_w^2$. The channel $h_{\mathrm{p},1}$ is considered to be independent of $x_{\mathrm{PT}}[n]$ and $w[n]$, thus, y_{ST} is also an independent and identically distributed (i.i.d.) random process.

Similar to (1), during data transmission, the discrete and real received signal at the SR conditioned on the detection probability $(\mathrm{P_d})$ and false alarm probability $(\mathrm{P_{fa}})$ is given by

$$y_{\mathrm{SR}}[n] = \begin{cases} h_{\mathrm{s}} \cdot x_{\mathrm{ST}}[n] + h_{\mathrm{p},2} \cdot x_{\mathrm{PT}}[n] + w[n] & : 1 - \mathrm{P_d} \\ h_{\mathrm{s}} \cdot x_{\mathrm{ST}}[n] + w[n] & : 1 - \mathrm{P_{fa}} \end{cases}, \tag{2}$$

where $x_{\mathrm{ST}}[n]$ corresponds to discrete and real sample transmitted by the ST. Further, $|h_{\mathrm{s}}|^2$ and $|h_{\mathrm{p},2}|^2$ represent the power gains for access and interference channels, cf. Fig. 1.

Sensing

Following the frame structure, ST performs sensing for a duration of τ_{sen}. The test statistics $\mathrm{T}(\mathbf{y})$ at the ST is evaluated as

$$\mathrm{T}(\mathbf{y}) = \frac{1}{\tau_{\mathrm{sen}} f_{\mathrm{s}}} \sum_{n=1}^{\tau_{\mathrm{sen}} f_{\mathrm{s}}} |y_{\mathrm{ST}}[n]|^2 \underset{\mathcal{H}_0}{\overset{\mathcal{H}_1}{\gtrless}} \mu, \tag{3}$$

where μ is the decision threshold and $\mathbf{y}$ is a vector with $\tau_{\mathrm{sen}} f_{\mathrm{s}}$ samples. $\mathrm{T}(\mathbf{y})$ represents a random variable, whereby the characterization of the distribution function depends on the underlying hypothesis. Corresponding to $\mathcal{H}_0$ and $\mathcal{H}_1$, $\mathrm{T}(\mathbf{y})$ follows a central chi-squared $(\mathcal{X}^2)$ distribution [33].

As a result, the detection probability ($\mathrm{P_d}$) and the false alarm probability ($\mathrm{P_{fa}}$) corresponding to (3) are determined as [21]

$$\mathrm{P_d}(\mu, \tau_{\text{sen}}, P_{\text{Rx,ST}}) = \Gamma\left(\frac{\tau_{\text{sen}} f_{\text{s}}}{2}, \frac{\tau_{\text{sen}} f_{\text{s}} \mu}{2 P_{\text{Rx,ST}}}\right), \tag{4}$$

$$\mathrm{P_{fa}}(\mu, \tau_{\text{sen}}) = \Gamma\left(\frac{\tau_{\text{sen}} f_{\text{s}}}{2}, \frac{\tau_{\text{sen}} f_{\text{s}} \mu}{2\sigma_w^2}\right), \tag{5}$$

where $P_{\text{Rx,ST}}$ is the power received over the sensing channel and $\Gamma(\cdot, \cdot)$ represents a regularized upper Gamma function [34].

Sensing-Throughput tradeoff

Following the characterization of $\mathrm{P_{fa}}$ and $\mathrm{P_d}$, Liang *et. al.* [14] established a tradeoff between the sensing time and secondary throughput (R_{s}) subject to a target detection probability ($\bar{\mathrm{P}}_{\text{d}}$). This tradeoff is represented as

$$R_{\text{s}}(\tilde{\tau}_{\text{sen}}) = \max_{\tau_{\text{sen}}} R_{\text{s}}(\tau_{\text{sen}}) = \frac{T - \tau_{\text{sen}}}{T}\Big[\mathrm{C}_0(1 - \mathrm{P_{fa}})\mathbb{P}(\mathcal{H}_0) + \mathrm{C}_1(1 - \mathrm{P_d})\mathbb{P}(\mathcal{H}_1)\Big], \tag{6}$$

$$\text{s.t. } \mathrm{P_d} \geq \bar{\mathrm{P}}_{\text{d}}, \tag{7}$$

$$\text{where } \mathrm{C}_0 = \log_2\left(1 + |h_{\text{s}}|^2 \frac{P_{\text{Tx,ST}}}{\sigma_w^2}\right) = \log_2\left(1 + \gamma_{\text{s}}\right) \tag{8}$$

$$\text{and } \mathrm{C}_1 = \log_2\left(1 + \frac{|h_{\text{s}}|^2 P_{\text{Tx,ST}}}{|h_{\text{p,2}}|^2 P_{\text{Tx,PT}} + \sigma_w^2}\right) = \log_2\left(1 + \frac{|h_{\text{s}}|^2 P_{\text{Tx,ST}}}{P_{\text{Rx,SR}}}\right) = \log_2\left(1 + \frac{\gamma_{\text{s}}}{\gamma_{\text{p,2}} + 1}\right), \tag{9}$$

where $\mathbb{P}(\mathcal{H}_0)$ and $\mathbb{P}(\mathcal{H}_1)$ are the probabilities of occurrence for the respective hypothesis, whereas $\gamma_{\text{p,2}}$ and γ_{s} correspond to signal to noise ratio for the links PT-SR and ST-SR, respectively. Moreover, $P_{\text{Tx,ST}}$ and $P_{\text{Tx,PT}}$ represent the transmit power at the PT and the ST, whereas $P_{\text{Rx,SR}}$ corresponds to the received power at the SR. In other words, using (6), the ST determines a suitable sensing time $\tau_{\text{sen}} = \tilde{\tau}_{\text{sen}}$, such that the throughput is maximized subject to a target detection probability, cf. (7). From the deployment perspective, the tradeoff depicted above has the following fundamental issues:

- Without the knowledge of the received power (sensing channel), it is not feasible to characterize $\mathrm{P_d}$. This leaves the characterization of the throughput (6) impossible and the constraint defined in (7) inappropriate.
- Moreover, the knowledge of the interacting channels is required at the ST, cf. (8) and (9) for characterizing the throughput in terms of C_0 and C_1 at the SR.

Taking into account these issues, it is not sensible to employ the performance analysis depicted by the ideal model for hardware implementation. In the subsequent section, we propose an estimation model that addresses these issues, thereby including the estimation of the sensing channel at the ST, and interference and access channels at the SR. Based on the proposed model, we then investigate the performance of the IS in terms of the sensing-throughput tradeoff.

III. Proposed Model

The inclusion of estimation of the interacting channels causes variations in the parameters $\mathrm{P_d}$, $\mathrm{C_0}$ and $\mathrm{C_1}$. Unless characterized, these variations may seriously degrade the performance of the hardware deployed. In this view, we include the estimation of the interacting channels in the system model, thereby characterizing the variations in $\mathrm{P_d}$, $\mathrm{C_0}$ and $\mathrm{C_1}$ by means of their their distribution functions $F_{\mathrm{P_d}}$, $F_{\mathrm{C_0}}$ and $F_{\mathrm{C_1}}$. By utilizing these expressions, we finally obtain a characterization of sensing-throughput tradeoff. To include channel estimation, we propose a frame structure that constitutes estimation τ_{est}, sensing τ_{sen} and data transmission $T-(\tau_{\mathrm{est}}+\tau_{\mathrm{sen}})$, where $\tau_{\mathrm{est}}, \tau_{\mathrm{sen}}$ correspond to time intervals and $\tau_{\mathrm{est}}+\tau_{\mathrm{sen}} < T$, cf. Fig. 2. In practice, the estimated values of the interacting channels are required for determining the suitable sensing time, hence, the sequence depicted in Fig. 2, whereby estimation followed by sensing is reasonable for the hardware deployment. In this regard, a low-rate feedback channel from the SR to the ST is required for the proposed model.

Besides that, particularly for the sensing channel, the samples used for estimation can be combined with the samples acquired for sensing ($\tau_{\mathrm{sen}}^{*} = \tau_{\mathrm{est}} + \tau_{\mathrm{sen}}$), thereby improving the performance of the detector at the ST. As τ_{sen}^{*} is dependent on $P_{\mathrm{Rx,ST}}$ or the state of $h_{\mathrm{p,1}}$ in particular, under this situation, τ_{sen}^{*} is lower bounded by τ_{est}, consequently translating $F_{\mathrm{P_d}}$ from a continuous function to a piecewise continuous function, thereby complicating the analytical tractability of $F_{\mathrm{P_d}}$. Hence, to simplify the analysis, in this work, we consider estimation and sensing as disjoint events in time. In this regard, the derived expressions based on our proposed model represents a lower performance bound. Next, in the following subsections, we present the estimation of the interacting channels.

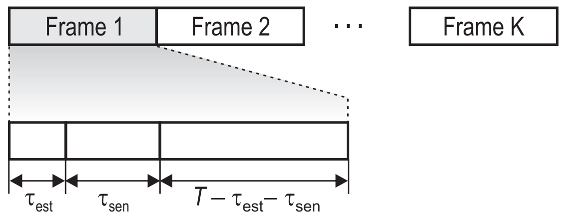

Fig. 2. Frame structure of interweave system with received power estimation.

Estimation of sensing channel ($h_{p,1}$)

Following the previous discussions, the ST acquires the knowledge of $h_{\text{p},1}$ by estimating its received power. The estimated received power is required for the characterization of P_{d}, thereby evaluating the detector performance.

Under $\mathcal{H}_1$, the received power estimated during the estimation phase at the ST is given as [8]

$$\hat{P}_{\text{Rx,ST}} = \frac{1}{\tau_{\text{est}} f_{\text{s}}} \sum_{n=1}^{\tau_{\text{est}} f_{\text{s}}} |y_{\text{ST}}[n]|^2. \tag{10}$$

$\hat{P}_{\text{Rx,ST}}$ determined in (10) using $\tau_{\text{est}} f_{\text{s}}$ samples follows a central chi-squared distribution $\mathcal{X}^2$ [33]. The cumulative distribution function of $\hat{P}_{\text{Rx,ST}}$ is given by

$$F_{\hat{P}_{\text{Rx,ST}}}(x) = \Gamma\left(\frac{\tau_{\text{est}} f_{\text{s}}}{2}, \frac{\tau_{\text{est}} f_{\text{s}} x}{2 P_{\text{Rx,ST}}}\right). \tag{11}$$

Estimation of access channel (h_s)

The signal received from the ST undergoes matched filtering and demodulation at the SR, hence, it is reasonable to employ pilot based estimation for h_{s}. Unlike received power estimation, pilot based estimation renders a direct estimation of the channel. Now, to accomplish pilot based estimation, the SR aligns itself to pilot symbols transmitted by the ST. Under $\mathcal{H}_0$, the discrete and real pilot symbols at the output of the demodulator is given by [24]

$$p[n] = \sqrt{E_{\text{s}}} h_{\text{s}} + w[n], \tag{12}$$

where E_{s} denotes the pilot energy. Without loss of generality, the pilot symbols are considered to be +1. The maximum likelihood estimate, representing a sample average of N_{s} pilot symbols, is given by [23]

$$h_{\text{s}} = \hat{h}_{\text{s}} + \underbrace{\frac{\sum_n^{N_{\text{s}}} p[n]}{2N_{\text{s}}}}_{\epsilon}, \tag{13}$$

where ϵ denotes the estimation error. The estimate $\hat{h}_{\mathrm{s}}$ is unbiased, efficient and achieves a Cramer-Rao bound with equality, with variance $\mathbb{E}\left[|h_{\mathrm{s}} - \hat{h}_{\mathrm{s}}|^2\right] = \sigma_w^2/(2N_{\mathrm{s}})$ [24]. Consequently, $\hat{h}_{\mathrm{s}}$ conditioned on h_{s} follows a Gaussian distribution.

$$\hat{h}_{\mathrm{s}}|h_{\mathrm{s}} \sim \mathcal{N}\left(h_{\mathrm{s}}, \frac{\sigma_w^2}{2N_{\mathrm{s}}}\right). \tag{14}$$

As a result, the power gain $|\hat{h}_{\mathrm{s}}|^2$ follows a non-central chi-squared ($\mathcal{X}_1^2$) distribution with 1 degree of freedom and non-centrality parameter $\lambda = \frac{2N_{\mathrm{s}}|h_{\mathrm{s}}|^2}{\sigma_w^2}$.

Estimation of interference channel ($h_{p,2}$)

In addition, analog to sensing channel, the SR performs received power estimation by listening to the transmission from the PT. The knowledge of $h_{\mathrm{p,2}}$ is required to characterize interference from the PT. Under $\mathcal{H}_1$, the discrete signal model at the SR is given as

$$y_{\mathrm{SR}}[n] = h_{\mathrm{p,2}} \cdot x_{\mathrm{PT}}[n] + w[n]. \tag{15}$$

The received power at the SR from the PT given by

$$\hat{P}_{\mathrm{Rx,SR}} = \frac{1}{N_{\mathrm{p,2}}} \sum_{n=1}^{N_{\mathrm{p,2}}} |y_{\mathrm{SR}}[n]|^2, \tag{16}$$

follows a $\mathcal{X}^2$ distribution, where $N_{\mathrm{p,2}}$ corresponds to the number of samples used for estimation.

Assumptions and Approximations

To simplify the analysis and sustain analytical tractability for the proposed model, several assumptions considered in the paper are summarized as follows:

- We consider that all transmitted signals are subjected to distance dependent path loss and small scale fading gain. With no loss of generality, we consider that the channel gains include distance dependent path loss and small scale gain. Moreover, the coherence time for the channel gain is considered to be greater than the frame duration[5].
- To ensure mathematical tractability of the proposed model, we consider disjoint sets of samples for estimation and sensing for a certain frame. However, in practice, it is possible

[5] In the scenarios where the coherence time exceeds the frame duration, in such cases our characterization depicts a lower performance bound.

to utilize the samples used in the estimation phase for sensing purpose as well, which leads to an improvement in the detector's performance in terms of the number of samples utilized for sensing.

- We assume perfect knowledge of the noise power in the system, however, the uncertainty in noise power can be captured as a bounded interval [21]. Inserting this interval in the derived expressions, cf. Section IV, the performance of the IS can be expressed in terms of the upper and the lower bounds.
- For all degrees of freedom, $\mathcal{X}_1^2$ distribution can be approximated as Gamma distribution [35]. The parameters of the Gamma distribution are obtained by matching the first two central moments to those of $\mathcal{X}_1^2$.
- Analog to [14], [16], [19], [20], the proposed model stipulates the knowledge of the underlying hypothesis at the ST and the SR. With the knowledge of occurrence probabilities $\mathbb{P}(\mathcal{H}_0)$ and $\mathbb{P}(\mathcal{H}_1)$ and subsequently applying PU traffic models proposed in [30]–[32], it is possible to acquire this knowledge with high probability.
- Considering a realistic situation, it is possible that SR might not accomplish estimation in each frame, under such circumstances, the ST utilizes the previous estimation value for the sensing-throughput analysis.

IV. Theoretical Analysis

At this stage, it is evident that the variation due to imperfect channel estimation translates to the variations of the performance parameters $\mathrm{P_d}, \mathrm{C_0}$ and $\mathrm{C_1}$, which are fundamental to sensing-throughput tradeoff. Below, we capture these variations by characterizing their cumulative distribution functions $F_{\mathrm{P_d}}$, $F_{\mathrm{C_0}}$ and $F_{\mathrm{C_1}}$, respectively.

Lemma 1: The cumulative distribution function of $\mathrm{P_d}$ is characterized as

$$F_{\mathrm{P_d}}(x) = 1 - \Gamma\left(\frac{\tau_{\mathrm{est}} f_{\mathrm{s}}}{2}, \frac{\tau_{\mathrm{est}} f_{\mathrm{s}} \tau_{\mathrm{sen}} f_{\mathrm{s}} \mu}{4 P_{\mathrm{Rx,ST}} \Gamma^{-1}\left(\frac{\tau_{\mathrm{sen}}}{2}, x\right)}\right), \tag{17}$$

where $\Gamma^{-1}(\cdot,\cdot)$ is inverse function of regularized upper Gamma function [34].

Proof: The cumulative distribution function of $\mathrm{P_d}$ is defined as

$$F_{\mathrm{P_d}}(x) = \mathbb{P}(\mathrm{P_d}(\mu, \tau_{\mathrm{sen}}, \hat{P}_{\mathrm{Rx,ST}}) \leq x). \tag{18}$$

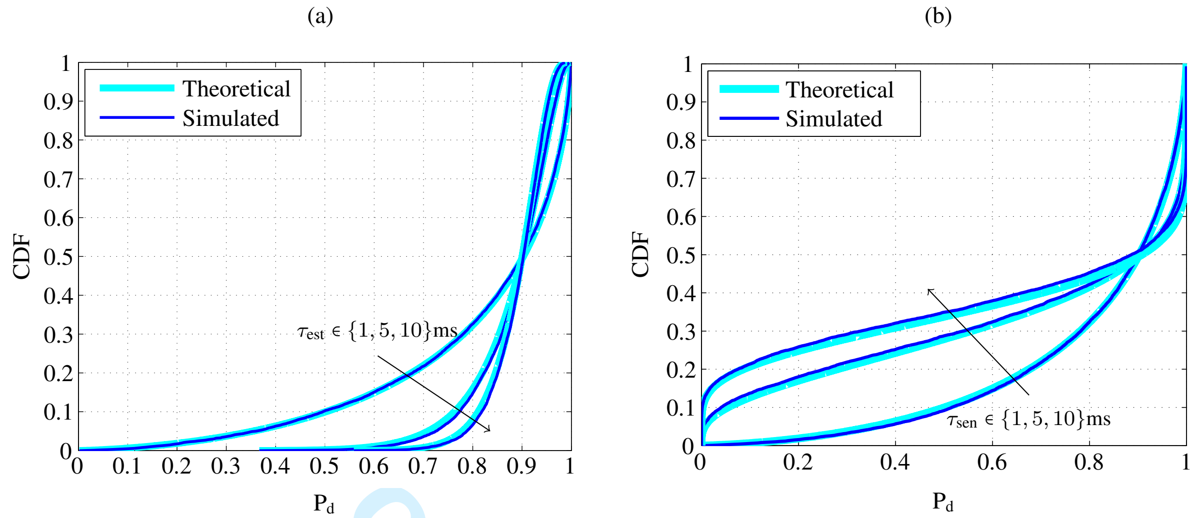

Fig. 3. CDF of $\mathrm{P_d}$ for different τ_{est} and τ_{sen}. (a) $\tau_{\mathrm{est}} \in \{1, 5, 10\}$ms and $\tau_{\mathrm{sen}} = 1$ ms, (b) $\tau_{\mathrm{est}} = 1$ ms and $\tau_{\mathrm{sen}} \in \{1, 5, 10\}$ms.

Using (4)

$$= \mathbb{P}\left(\Gamma\left(\frac{\tau_{\mathrm{sen}} f_{\mathrm{s}}}{2}, \frac{\tau_{\mathrm{est}} f_{\mathrm{s}} \mu}{2\hat{P}_{\mathrm{Rx,ST}}}\right) \leq x\right), \tag{19}$$

$$= 1 - \mathbb{P}\left(\hat{P}_{\mathrm{Rx,ST}} \leq \frac{\mu \tau_{\mathrm{sen}} f_{\mathrm{s}}}{2\Gamma^{-1}\left(\frac{\tau_{\mathrm{sen}} f_{\mathrm{s}}}{2}, x\right)}\right). \tag{20}$$

Replacing the cumulative distribution function of $\hat{P}_{\mathrm{Rx,ST}}$ in (20), we obtain an expression of $F_{\mathrm{P_d}}$.

■

Lemma 2: The cumulative distribution function of $\mathrm{C_0}$ is defined as

$$F_{\mathrm{C_0}}(x) = \int_0^x f_{\mathrm{C_0}}(t) dt, \tag{21}$$

where

$$f_{\mathrm{C_0}}(x) = 2^x \ln 2 \frac{(2^x - 1)^{a_1 - 1}}{\Gamma(a_1) b_1^{a_1}} \exp\left(-\frac{2^x - 1}{b_1}\right), \tag{22}$$

and

$$a_1 = \frac{\left(\frac{\sigma_w^4}{2N_{\mathrm{s}} P_{\mathrm{Tx,ST}}} + |h_{\mathrm{s}}|^2\right)^2}{\frac{\sigma_w^4}{2N_{\mathrm{s}} P_{\mathrm{Tx,ST}}}\left(2\frac{\sigma_w^4}{2N_{\mathrm{s}} P_{\mathrm{Tx,ST}}} + 4|h_{\mathrm{s}}|^2\right)} \text{ and } b_1 = \frac{\frac{\sigma_w^4}{2N_{\mathrm{s}} P_{\mathrm{Tx,ST}}}\left(2\frac{\sigma_w^4}{2N_{\mathrm{s}} P_{\mathrm{Tx,ST}}} + 4|h_{\mathrm{s}}|^2\right)}{\left(\frac{\sigma_w^4}{2N_{\mathrm{s}} P_{\mathrm{Tx,ST}}} + |h_{\mathrm{s}}|^2\right)}. \tag{23}$$

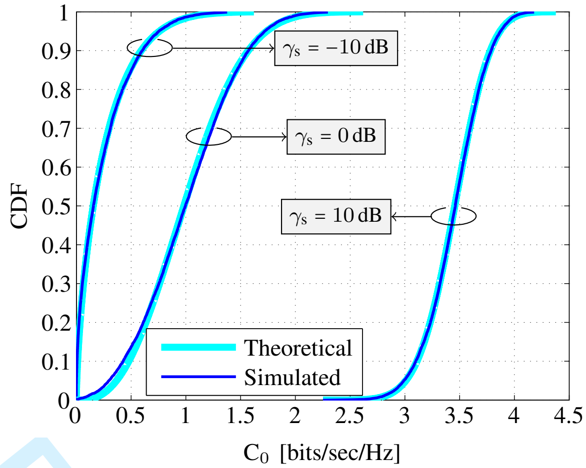

Fig. 4. CDF of C_0 for different values of $\gamma_{\mathrm{s}} \in \{-10, 0, 10\}$dB.

Proof: Following the probability density function (pdf) of $|\hat{h}_{\mathrm{s}}|^2$ in (14), the pdf $|\hat{h}_{\mathrm{s}}|^2 \frac{P_{\mathrm{Tx,ST}}}{\sigma_w^2}$ is given by

$$f_{\frac{|\hat{h}_{\mathrm{s}}|^2 P_{\mathrm{Tx,ST}}}{\sigma_w^2}}(x) = \frac{2N_{\mathrm{s}} P_{\mathrm{Tx,ST}}}{\sigma_w^4} \frac{1}{2} \exp\left[-\frac{1}{2}\left(x \frac{\sigma_w^4}{2N_{\mathrm{s}} P_{\mathrm{Tx,ST}}} + \lambda\right)\right]\left(\frac{x}{\lambda} \frac{\sigma_w^4}{2N_{\mathrm{s}} P_{\mathrm{Tx,ST}}}\right)^{\frac{N_{\mathrm{s}}}{4}-\frac{1}{2}}$$
$$\times I_{\frac{N_{\mathrm{s}}}{2}-1}\left(\sqrt{\lambda x \frac{\sigma_w^4}{2N_{\mathrm{s}} P_{\mathrm{Tx,ST}}}}\right),$$

where $I_{(\cdot)}(\cdot)$ represents the modified Bessel function of first kind [34]. Approximating $\mathcal{X}_1^2(\cdot,\cdot)$ with Gamma distribution $\Gamma(a_1, b_1)$ [35] gives

$$f_{\frac{|\hat{h}_{\mathrm{s}}|^2 P_{\mathrm{Tx,ST}}}{\sigma_w^2}} \approx \frac{1}{\Gamma(a_1)} \frac{x^{a_1-1}}{b_1^{a_1}} \exp\left(-\frac{x}{b_1}\right), \tag{24}$$

where the parameters a_1 and b_1 in (24) are determined by comparing the first two central moments of the two distributions. Finally, by substituting the expression of C_0 in (8) yields (22). ∎

Lemma 3: The cumulative distribution function of C_1 is given by

$$F_{\mathrm{C}_1}(x) = \int_0^x f_{\mathrm{C}_1}(t) dt, \tag{25}$$

where

$$f_{\mathrm{C}_1}(x) = 2^x \ln 2 \frac{(2^x - 1)^{a_1-1} \Gamma(a_1 + a_2)}{\Gamma(a_1)\Gamma(a_2) b_1^{a_1} b_2^{a_2}} \left(\frac{1}{b_2} + \frac{2^x - 1}{b_1}\right), \tag{26}$$

and

$$a_2 = \frac{N_{\mathrm{p},2}}{2} \text{ and } b_2 = \frac{2P_{\mathrm{Rx,ST}}}{\sigma_w^2 N_{\mathrm{p},2}}, \tag{27}$$

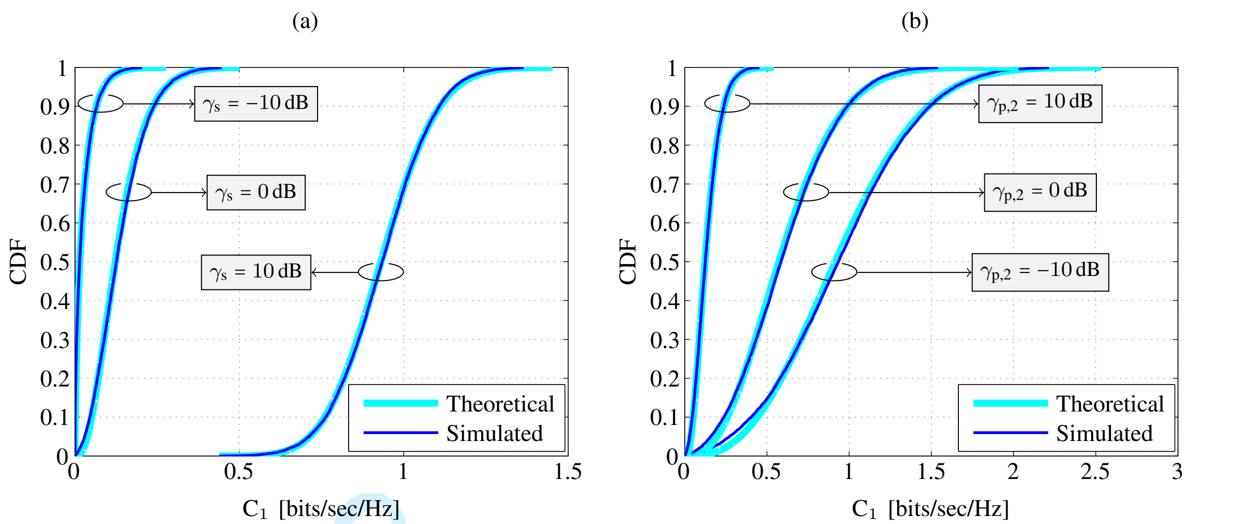

Fig. 5. CDF of C_1 for different γ_s and $\gamma_{p,2}$. (a) $\gamma_s \in \{-10, 0, 10\}$dB and $\gamma_{p,2} = 10$ dB, (b) $\gamma_s = 0$ dB and $\gamma_{p,2} \in \{-10, 0, 10\}$dB.

where a_1 and b_1 are defined in (23).

Proof: For simplification, we break down the expression $\left(\frac{|\hat{h}_s|^2 P_{\text{Tx,ST}}}{\hat{P}_{\text{Rx,SR}}}\right)$ in (9), as $E_1 = \left(\frac{|\hat{h}_s|^2 P_{\text{Tx,ST}}}{\sigma_w^2}\right)$ and $E_2 = \left(\frac{\hat{P}_{\text{Rx,SR}}}{\sigma_w^2}\right)$, where $\mathrm{C}_1 = \log_2\left(1 + \frac{E_1}{E_2}\right)$. The pdf of the expression E_1 is determined in (24). Following the characterization $\hat{P}_{\text{Rx,SR}}$ in (16), the pdf of E_2 is determined as

$$f_{\frac{\hat{P}_{\text{Rx,SR}}}{\sigma_w^2}} = \frac{N_{p,2}\sigma_w^2}{P_{\text{Rx,ST}}} \frac{1}{2^{\frac{N_{p,2}}{2}} \Gamma\left(\frac{N_{p,2}}{2}\right)} \left(x \frac{N_{p,2}\sigma_w^2}{P_{\text{Rx,ST}}}\right)^{\frac{N_{p,2}}{2}-1} \exp\left(-x \frac{N_{p,2}\sigma_w^2}{2P_{\text{Rx,ST}}}\right). \tag{28}$$

Using the characterizations of pdfs $f_{\frac{|\hat{h}_s|^2 P_{\text{Tx,ST}}}{\sigma_w^2}}$ and $f_{\frac{\hat{P}_{\text{Rx,SR}}}{\sigma_w^2}}$, we apply Mellin transform [36] to determine the pdf of $\frac{E_1}{E_2}$ as

$$f_{\frac{|\hat{h}_s|^2 P_{\text{Tx,ST}}}{\sigma_w^2} \Big/ \frac{\hat{P}_{\text{Rx,SR}}}{\sigma_w^2}}(x) = \frac{x^{a_1-1}\Gamma(a_1+a_2)}{\Gamma(a_1)\Gamma(a_2) b_1^{a_1} b_2^{a_2}} \left(\frac{1}{b_2} + \frac{x}{b_1}\right). \tag{29}$$

Finally, substituting the expression $\frac{E_1}{E_2}$ in C_1 yields (26). ■

The theoretical expressions of the distribution functions depicted in Lemma 1, Lemma 2 and Lemma 3 are validated by means of simulations in Fig. 3, Fig. 4 and Fig. 5, respectively, with different choices of system parameters, these include $\tau_{\text{est}} \in \{1, 5, 10\}$ms, $\tau_{\text{sen}} = \{1, 5, 10\}$ms, $\gamma_s \in \{-10, 0, 10\}$dB and $\gamma_{p,2} \in \{-10, 0, 10\}$dB.

Sensing-throughput tradeoff

Here, we establish sensing-throughput tradeoff for the estimation model that includes estimation time and incorporates variations in the performance parameter. Most importantly, by capturing these variations, we establish two new PU constraints at the PR, namely, an average constraint and an outage constraint on the detection probability. These constraints restrain the harmful interference at the PR. Based on these constraints and a certain choice of estimation time τ_{est}, we characterize the sensing-throughput tradeoff for the IS.

Theorem 1: Subject to an average constraint on P_{d} at the PR, the sensing-throughput tradeoff is given by

$$R_{\text{s}}(\tilde{\tau}_{\text{sen}}) = \max_{\tau_{\text{sen}}} \mathbb{E}_{\text{P}_{\text{d}},\text{C}_0,\text{C}_1}\left[R_{\text{s}}(\tau_{\text{sen}})\right],$$
$$= \frac{T-\tau_{\text{sen}}-\tau_{\text{est}}}{T}\Bigg[\mathbb{E}_{\text{C}_0}\left[\text{C}_0\right](1-\text{P}_{\text{fa}})\mathbb{P}(\mathcal{H}_0) + \mathbb{E}_{\text{C}_1}\left[\text{C}_1\right](1-\mathbb{E}_{\text{P}_{\text{d}}}\left[\text{P}_{\text{d}}\right])\mathbb{P}(\mathcal{H}_1)\Bigg], \quad (30)$$
$$\text{s.t. } \mathbb{E}_{\text{P}_{\text{d}}}\left[\text{P}_{\text{d}}\right] \leq \bar{\text{P}}_{\text{d}}, \quad (31)$$

where $\mathbb{E}_{\text{P}_{\text{d}}}[\cdot]$ represents the expectation with respect to P_{d}, $\mathbb{E}_{\text{P}_{\text{d}},\text{C}_0,\text{C}_1}[\cdot]$ denotes the expectation with respect to P_{d}, C_0 and C_1. Unlike (7), $\bar{\text{P}}_{\text{d}}$ in (30) represents the constraint on expected detection probability.

Proof: The proof of Theorem 1 is included in the proof of Theorem 2. ■

Theorem 2: Subject to an outage constraint on P_{d} at the PR, the sensing-throughput tradeoff is given by

$$R_{\text{s}}(\tilde{\tau}_{\text{sen}}) = \max_{\tau_{\text{sen}}} \mathbb{E}_{\text{P}_{\text{d}},\text{C}_0,\text{C}_1}\left[R_{\text{s}}(\tau_{\text{sen}})\right],$$
$$= \frac{T-\tau_{\text{sen}}-\tau_{\text{est}}}{T}\Bigg[\mathbb{E}_{\text{C}_0}\left[\text{C}_0\right](1-\text{P}_{\text{fa}})\mathbb{P}(\mathcal{H}_0) + \mathbb{E}_{\text{C}_1}\left[\text{C}_1\right](1-\mathbb{E}_{\text{P}_{\text{d}}}\left[\text{P}_{\text{d}}\right])\mathbb{P}(\mathcal{H}_1)\Bigg], \quad (32)$$
$$\text{s.t. } \mathbb{P}(\text{P}_{\text{d}} \leq \bar{\text{P}}_{\text{d}}) \leq \kappa, \quad (33)$$

where κ represents the outage constraint.

Proof: In order to solve the constrained optimization problems illustrated in Theorem 1 and Theorem 2, the following approach is considered. As a first step, an underlying constraint is employed to determine μ as a function of the τ_{sen} and τ_{est}.

For the average constraint, the expression $\mathbb{E}_{\text{P}_{\text{d}}}\left[\text{P}_{\text{d}}\right]$ in (31) did not lead to a closed form expression, consequently, no analytical expression of μ is obtained. In this context, we procure μ for the average constraint numerically from (31).

Next, we determine μ based on the outage constraint. This is accomplished by combining the expression of $F_{\mathrm{P_d}}$ in (17) with the outage constraint (33)

$$P(\mathrm{P_d} \le \bar{\mathrm{P}}_\mathrm{d}) = F_{\mathrm{P_d}}(\bar{\mathrm{P}}_\mathrm{d}) \le \kappa. \tag{34}$$

Rearranging (34) gives

$$\mu \ge \frac{4P_{\mathrm{Rx,ST}}\Gamma^{-1}\left(1-\kappa, \frac{\tau_{\mathrm{est}} f_\mathrm{s}}{2}\right)\Gamma^{-1}\left(1-\bar{\mathrm{P}}_\mathrm{d}, \frac{\tau_{\mathrm{sen}} f_\mathrm{s}}{2}\right)}{\tau_{\mathrm{est}}\tau_{\mathrm{sen}}(f_\mathrm{s})^2}. \tag{35}$$

Upon replacing the respective thresholds in $\mathrm{P_d}$ and $\mathrm{P_{fa}}$ and evaluating the expectation over $\mathrm{P_d}$, C_0 and C_1 using the distribution functions characterized in Lemma 1, Lemma 2 and Lemma 3, we determine the expected throughput as a function of sensing and estimation time. ■

As a consequence, for a certain estimation time, the sensing-throughput tradeoff that depicts the variation of expected throughput against the sensing time is established based on the average and outage constraints. In contrast to the ideal model, the sensing-throughput tradeoff substantiated by the estimation model, which incorporates the channel knowledge is qualified for characterizing the performance of IS.

Corollary 1: Herein, based on the estimation model, we establish a fundamental relation between estimation time (regulates the variation in the detection probability according to the PU constraint), sensing time (represents the detector performance) and achievable throughput, this relationship is characterized as estimation-sensing-throughput tradeoff. Based on this tradeoff, we determine the suitable estimation $\tau_{\mathrm{est}} = \tilde{\tau}_{\mathrm{est}}$ and sensing time $\tau_{\mathrm{sen}} = \tilde{\tau}_{\mathrm{sen}}$ that attains a maximum achievable throughput $R_\mathrm{s}(\tilde{\tau}_{\mathrm{est}}, \tilde{\tau}_{\mathrm{sen}})$ for the IS.

V. Numerical Results

Here, we investigate the performance of the IS based on the proposed model. To accomplish this: (i) we perform simulations to validate the expressions obtained, (ii) we analyze the performance loss incurred due to the estimation. In this regard, we consider the ideal model for benchmarking and evaluating the performance loss, (iii) we establish mathematical justification to the considered approximations. Although, the expressions derived using our sensing-throughput analysis are general and applicable to all CR systems, the parameters are selected in such a way that they closely relate to the deployment scenario described in Fig. 1. Unless stated explicitly, the choice of the parameters given in Table II is considered for the analysis.

TABLE II

PARAMETERS FOR NUMERICAL ANALYSIS

Parameter	Value
f_s	1 MHz
$h_{p,1}, h_{p,2}$	−100 dB
h_s	−80 dB
T	100 ms
$\bar{P}_d$	0.9,
κ	0.05
σ_w^2	−100 dBm
$\gamma_{p,1}$	−10 dB
$\gamma_{p,2}$	−10 dB
γ_s	10 dB
$\sigma_x^2 = P_{Tx,PT}$	−10 dBm
$P_{Tx,ST}$	−10 dBm
$\mathbb{P}(\mathcal{H}_1) = 1 - \mathbb{P}(\mathcal{H}_0)$	0.2
τ_{est}	5 ms
N_s	10
$N_{p,2}$	1000

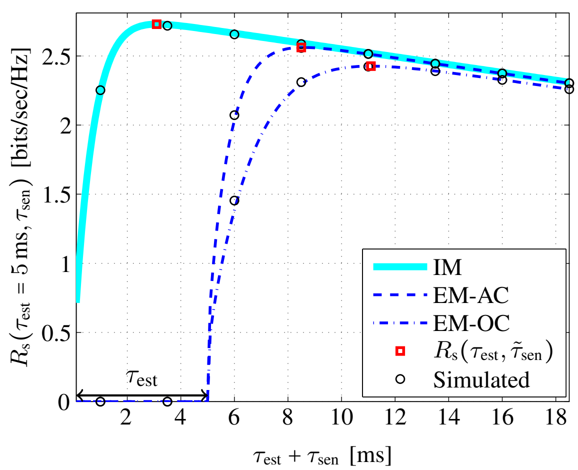

Fig. 6. Sensing-throughput tradeoff for the ideal and estimation models with $\gamma_{p,1} = -10$ dB, $\tau_{est} = 5$ ms and $\kappa = 0.05$.

Firstly, we analyze the performance of the IS in terms of sensing-throughput tradeoff corresponding to the ideal model (IM) and estimation model (EM) by fixing $\tau_{est} = 5$ ms, cf. Fig. 6. In contrast to constraint on P_d for the ideal model, we employ average constraint (EM-AC) and

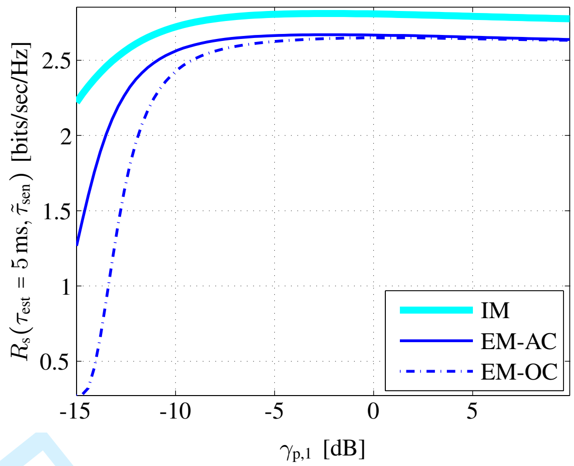

Fig. 7. Achievable throughput versus the $\gamma_{p,1}$ with $\tau_{est} = 5\,ms$.

outage constraint (EM-OC) for the proposed estimation model. With the inclusion of received power estimation in the frame structure, the ST procures no throughput at the SR for the interval τ_{est}. For the given cases, namely, IM, EM-AC and EM-OC, a suitable sensing time that results in a maximum throughput $R_s(\tau_{est} = 5\,ms, \tilde{\tau}_{sen})$ is determined. Hence, a performance degradation is depicted in terms of the achievable throughput, cf. Fig. 6. For $\kappa = 0.05$, it is observed that the outage constraint is more sensitive to the performance loss in comparison to average constraint. It is clear that the analysis illustrated Fig. 6 is obtained for a certain choice of system parameters, particularly $\gamma_{p,1} = -10\,dB$, $\tau_{est} = 5\,ms$ and $\kappa = 0.05$. To acquire more insights, we consider the effect of variation of these parameters on the performance of IS, subsequently.

Hereafter, for the analysis, we consider the theoretical expressions and choose to operate at suitable sensing time. Next, we determine the variations of the achievable throughput against the received signal to noise ratio $\gamma_{p,1}$ at the ST with $\tau_{est} = 5\,ms$, cf. Fig. 7. For $\gamma_{p,1} < -5\,dB$, the estimation model incurs a significant performance loss. This clearly reveals that the ideal model overestimates the performance of IS. Hence, it is perceived that despite loss in performance, the estimation model is capable of precluding interference at the PR, hence, assuring reliability to the system.

Upon maximizing the secondary throughput, it is interesting to analyze the variation of achievable throughput with the estimation time. Corresponding to the estimation model, Fig. 8 illustrates a tradeoff among the estimation time, the sensing time and the throughput, cf. Corollary

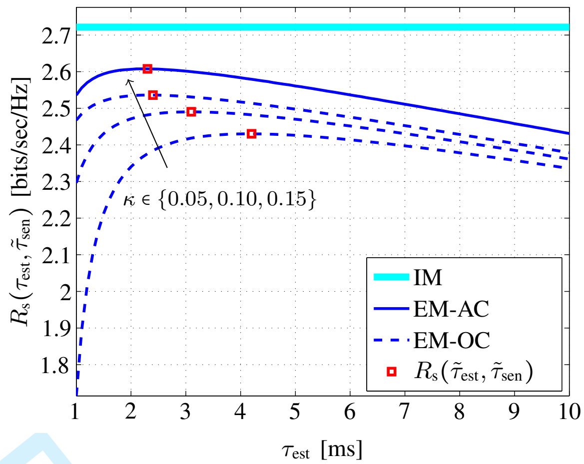

Fig. 8. Estimation-throughput tradeoff for the average and outage constraints with $\gamma_{p,1} = -10\,$dB, where the throughput is maximized over the sensing time, $R_s(\tau_{est}, \tilde{\tau}_{sen})$. Estimation-throughput tradeoff is utilized to determine a suitable estimation time $\tilde{\tau}_{est}$ that maximizes the throughput, $R_s(\tilde{\tau}_{est}, \tilde{\tau}_{sen})$.

1. This can be explained from the fact that low values of estimation time result in large variation in P_d. To counteract and satisfy the average and outage constraints, the corresponding thresholds shift to a lower value. This causes an increase in P_{fa}, thereby increasing the sensing-throughput curvature. As a result, the suitable sensing time is obtained at a higher value. However, beyond a certain value ($\tilde{\tau}_{est}$), a further increase in estimation time slightly contributes to performance improvement and largely consumes the time resources. As a consequence to the estimation-sensing-throughput tradeoff, we determine the suitable estimation time that yields an achievable throughput $R_s(\tilde{\tau}_{est}, \tilde{\tau}_{sen})$. Besides that, we consider the variation of achievable throughput for different values of the outage constraint, cf. Fig. 8. It is observed that for the selected choice of κ, the outage constraint is severe as compared to the average constraint, hence, results in a lower throughput. Thus, depending on the nature of policy (aggressive or conservative) followed by the regulatory bodies towards interference at the primary system, it is possible to define κ accordingly during the system design.

To procure further insights, we investigate the variations of expected P_d and P_{fa} with the estimation time. From Fig. 9a, it is observed that the expected P_d corresponding to the outage constraint is strictly above the desired level $\bar{P}_d$ for all values of estimation time, however, for lower values of estimation time, this margin reduces. This is based on the fact that lower estimation time shifts the probability mass of P_d, to a lower value, cf. Fig. 3a. Besides that, based on the previous discussion, it was analyzed that P_{fa} accounts for a large contribution to the throughput.

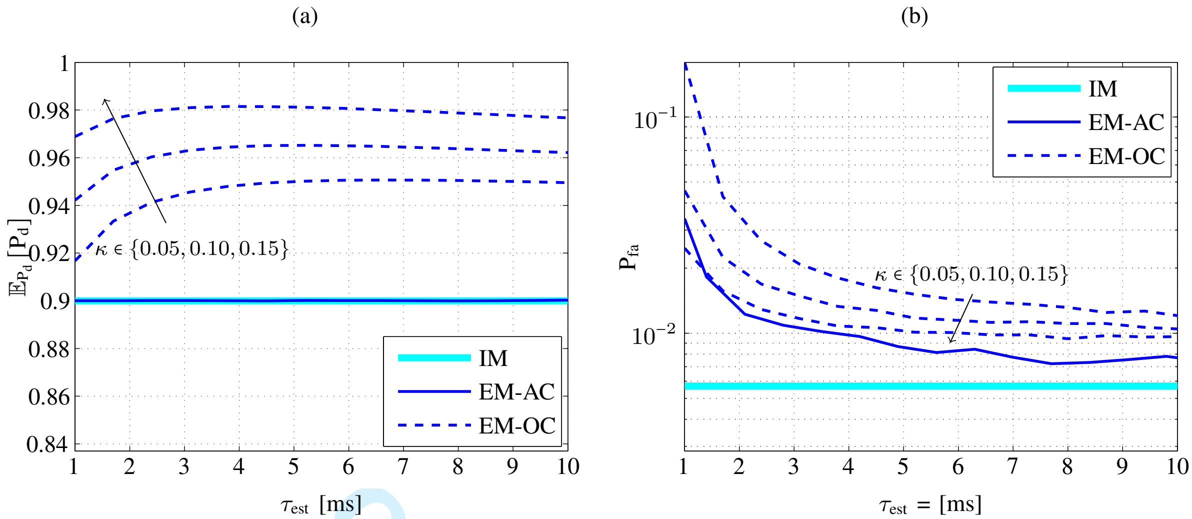

Fig. 9. Variation of $\mathbb{E}_{\mathrm{P_d}}[\mathrm{P_d}]$ and $\mathrm{P_{fa}}$ versus the τ_{est}, where the secondary throughput is maximized over the sensing time, $R_{\mathrm{s}}(\tau_{\mathrm{est}}, \tilde{\tau}_{\mathrm{sen}})$. (a) Expected $\mathrm{P_d}$ versus τ_{est}, (b) $\mathrm{P_{fa}}$ versus τ_{est}.

According to Fig. 9b, $\mathrm{P_{fa}}$ witnesses a large improvement in performance in the regime $\tau_{\mathrm{est}} \leq 3\,\mathrm{ms}$, however, saturates in the regime $\tau_{\mathrm{est}} \geq 3\,\mathrm{ms}$, thus, provides further justification to the variation of $R_{\mathrm{s}}(\tau_{\mathrm{est}}, \tilde{\tau}_{\mathrm{sen}})$ against τ_{est} characterized as estimation-sensing-throughput tradeoff depicted in Fig. 8.

VI. Conclusion

In this paper, we have investigated the performance of cognitive radio as an interweave system from a deployment perspective. It has been argued that the knowledge of the interacting channels is a key aspect that enables the performance characterization of the interweave system in terms of sensing-throughput tradeoff. In this regard, a novel model that facilitates channel estimation and captures the effect of estimation in the system model has been proposed. As a major outcome of the analysis, it has been justified that the existing model, illustrating an ideal scenario, overestimates the performance of the interweave system, hence, less suitable for deployment. Moreover, it has been indicated that the variation induced in the system, specially in the detection probability may severely degrade the performance of the primary system. To overcome this situation, average and outage constraints as primary user constraints have been employed. As a consequence, for the proposed estimation model, novel expressions for sensing-throughput tradeoff based on the mentioned constraints have been established. More importantly, by analyzing the estimation-sensing-throughput tradeoff, suitable estimation time and sensing time that maximizes the secondary throughput have been determined. In our future work, we plan to extend the proposed analysis for the hybrid cognitive radio system that combines the advantages of interweave and underlay techniques.

REFERENCES

[1] A. Kaushik, S. K. Sharma, S. Chatzinotas, B. Ottersten, and F. K. Jondral, "Sensing-Throughput Tradeoff for Cognitive Radio Systems with Unknown Received Power," in *10th International Conference on Cognitive Radio Oriented Wireless Networks and Communications (CROWNCOM)*, April 2015.

[2] J. Andrews, S. Buzzi, W. Choi, S. Hanly, A. Lozano, A. Soong, and J. Zhang, "What Will 5G Be?" *IEEE Journal on Selected Areas in Communications*, vol. 32, no. 6, pp. 1065–1082, June 2014.

[3] T. Rappaport, S. Sun, R. Mayzus, H. Zhao, Y. Azar, K. Wang, G. Wong, J. Schulz, M. Samimi, and F. Gutierrez, "Millimeter Wave Mobile Communications for 5G Cellular: It Will Work!" *IEEE Access*, vol. 1, pp. 335–349, 2013.

[4] J. Mitola and G. Q. Jr. Maguire, "Cognitive radio: making software radios more personal," *IEEE Personal Communications*, vol. 6, no. 4, pp. 13–18, August 1999.

[5] A. Goldsmith, S. Jafar, I. Maric, and S. Srinivasa, "Breaking Spectrum Gridlock With Cognitive Radios: An Information Theoretic Perspective," *Proceedings of the IEEE*, vol. 97, no. 5, pp. 894–914, May 2009.

[6] S. Sharma, T. Bogale, S. Chatzinotas, B. Ottersten, L. Le, and X. Wang, "Cognitive Radio Techniques under Practical Imperfections: A Survey," *IEEE Communications Surveys Tutorials*, vol. PP, no. 99, pp. 1–1, 2015.

[7] E. Axell, G. Leus, E. Larsson, and H. Poor, "Spectrum Sensing for Cognitive Radio : State-of-the-Art and Recent Advances," *IEEE Signal Processing Magazine*, vol. 29, no. 3, pp. 101–116, May 2012.

[8] H. Urkowitz, "Energy detection of unknown deterministic signals," *Proceedings of the IEEE*, vol. 55, no. 4, pp. 523 – 531, april 1967.

[9] V. Kostylev, "Energy detection of a signal with random amplitude," in *IEEE ICC*, vol. 3, 2002, pp. 1606–1610.

[10] F. Digham, M.-S. Alouini, and M. K. Simon, "On the energy detection of unknown signals over fading channels," in *IEEE ICC*, vol. 5, May 2003, pp. 3575–3579.

[11] S. Herath, N. Rajatheva, and C. Tellambura, "Unified Approach for Energy Detection of Unknown Deterministic Signal in Cognitive Radio Over Fading Channels," in *IEEE ICC Workshops*, June 2009, pp. 1–5.

[12] A. Mariani, A. Giorgetti, and M. Chiani, "Energy detector design for cognitive radio applications," in *2010 International Waveform Diversity and Design Conference (WDD)*, Aug 2010, pp. 053–057.

[13] E. Peh and Y.-C. Liang, "Optimization for cooperative sensing in cognitive radio networks," in *IEEE Wireless Communications and Networking Conference (WCNC)*, March 2007, pp. 27–32.

[14] Y.-C. Liang, Y. Zeng, E. Peh, and A. T. Hoang, "Sensing-Throughput Tradeoff for Cognitive Radio Networks," *IEEE Transactions on Wireless Communications*, vol. 7, no. 4, pp. 1326–1337, April 2008.

[15] S. Sharma, S. Chatzinotas, and B. Ottersten, "A hybrid cognitive transceiver architecture: Sensing-throughput tradeoff," in *CROWNCOM*, Jun. 2014.

[16] H. Pradhan, S. Kalamkar, and A. Banerjee, "Sensing-Throughput Tradeoff in Cognitive Radio With Random Arrivals and Departures of Multiple Primary Users," *IEEE Communications Letters*, vol. 19, no. 3, pp. 415–418, March 2015.

[17] M. K. Simon and M. S. Alouini, *Digital Communication over Fading Channels: A Unified Approach to Performance Analysis*, 1st ed. New York: Wiley, 2000.

[18] A. Kaushik, M. R. Raza, and F. K. Jondral, "On the Deployment of Cognitive Relay as Underlay Systems," in *CROWNCOM*, Jun. 2014.

[19] M. Cardenas-Juarez and M. Ghogho, "Spectrum Sensing and Throughput Trade-off in Cognitive Radio under Outage Constraints over Nakagami Fading," *IEEE Communications Letters*, vol. 15, no. 10, pp. 1110–1113, October 2011.

[20] Y. Sharkasi, M. Ghogho, and D. McLernon, "Sensing-throughput tradeoff for OFDM-based cognitive radio under outage constraints," in *ISWCS*, Aug 2012, pp. 66–70.

[21] R. Tandra and A. Sahai, "SNR Walls for Signal Detection," *IEEE Journal of Selected Topics in Signal Processing*, vol. 2, no. 1, pp. 4–17, Feb 2008.

[22] M. Gans, "The Effect of Gaussian Error in Maximal Ratio Combiners," *IEEE Transactions on Communication Technology*, vol. 19, no. 4, pp. 492–500, August 1971.

[23] W. Gifford, M. Win, and M. Chiani, "Diversity with practical channel estimation," *IEEE Transactions on Wireless Communications*, vol. 4, no. 4, pp. 1935–1947, July 2005.

[24] ——, "Antenna subset diversity with non-ideal channel estimation," *IEEE Transactions on Wireless Communications*, vol. 7, no. 5, pp. 1527–1539, May 2008.

[25] R. Annavajjala and L. Milstein, "Performance analysis of linear diversity-combining schemes on Rayleigh fading channels with binary signaling and Gaussian weighting errors," *IEEE Transactions on Wireless Communications*, vol. 4, no. 5, pp. 2267–2278, Sept 2005.

[26] H. Suraweera, P. Smith, and M. Shafi, "Capacity limits and performance analysis of cognitive radio with imperfect channel knowledge," *IEEE Transactions on Vehicular Technology*, vol. 59, no. 4, pp. 1811–1822, May 2010.

[27] H. Kim, H. Wang, S. Lim, and D. Hong, "On the Impact of Outdated Channel Information on the Capacity of Secondary User in Spectrum Sharing Environments," *IEEE Transactions on Wireless Communications*, vol. 11, no. 1, pp. 284–295, January 2012.

[28] A. Kaushik, S. K. Sharma, S. Chatzinotas, B. Ottersten, and F. K. Jondral, "Estimation-Throughput Tradeoff for Underlay Cognitive Radio Systems," *IEEE ICC 2015 - Cognitive Radio and Networks Symposium (ICC'15 (12) CRN)*, Jun. 2015.

[29] A. Kaushik, M. Mueller, and F. K. Jondral, "Cognitive Relay: Detecting Spectrum Holes in a Dynamic Scenario," in *ISWCS*, Apr. 2013, pp. 1–2.

[30] T. Wang, Y. Chen, E. Hines, and B. Zhao, "Analysis of effect of primary user traffic on spectrum sensing performance," in *Fourth International Conference on Communications and Networking in China*, Aug 2009, pp. 1–5.

[31] L. Tang, Y. Chen, E. Hines, and M.-S. Alouini, "Effect of Primary User Traffic on Sensing-Throughput Tradeoff for Cognitive Radios," *IEEE Transactions on Wireless Communications*, vol. 10, no. 4, pp. 1063–1068, April 2011.

[32] B. Zhao, Y. Chen, C. He, and L. Jiang, "Performance analysis of spectrum sensing with multiple primary users," *IEEE Transactions on Vehicular Technology*, vol. 61, no. 2, pp. 914–918, Feb 2012.

[33] S. Kay, *Fundamentals of Statistical Signal Processing: Detection theory*, ser. Prentice Hall Signal Processing Series. Prentice-Hall PTR, 1998.

[34] I. S. Gradshteyn and I. M. Ryzhik, *Table of Integrals, Series, and Products*, 6th ed. San Diego, CA: Academic Press., 2000.

[35] M. Abramowitz and I. A. Stegun, *Handbook of Mathematical Functions with Formulas, Graphs, and Mathematical Tables*, ninth Dover printing, tenth GPO printing ed. New York: Dover, 1964.

[36] F. W. J. Olver, D. W. Lozier, R. F. Boisvert, and C. W. Clark, Eds., *NIST Handbook of Mathematical Functions*. New York, NY: Cambridge University Press, 2010.

Sensing-Throughput Tradeoff for Interweave Cognitive Radio System: A Deployment-Centric Viewpoint

Ankit Kaushik*, *Student Member, IEEE*, Shree Krishna Sharma†, *Member, IEEE*,
Symeon Chatzinotas†, *Senior Member, IEEE*, Björn Ottersten†, *Fellow, IEEE*,
Friedrich K. Jondral* *Senior Member, IEEE*

***Abstract*—Secondary access to the licensed spectrum is viable only if interference is avoided at the primary system. In this regard, different paradigms have been conceptualized in the existing literature. Of these, Interweave Systems (ISs) that employ spectrum sensing have been widely investigated. Baseline models investigated in the literature characterize the performance of IS in terms of a sensing-throughput tradeoff, however, this characterization assumes the knowledge of the involved channels at the secondary transmitter, which is unavailable in practice. Motivated by this fact, we establish a novel approach that incorporates channel estimation in the system model, and consequently investigate the impact of imperfect channel estimation on the performance of the IS. More particularly, the variation induced in the detection probability affects the detector's performance at the secondary transmitter, which may result in severe interference at the primary users. In this view, we propose to employ average and outage constraints on the detection probability, in order to capture the performance of the IS. Our analysis reveals that with an appropriate choice of the estimation time determined by the proposed model, the degradation in performance of the IS can be effectively controlled, and subsequently the achievable secondary throughput can be significantly enhanced.**

***Index Terms*—Cognitive radio, Interweave System, Sensing-throughput tradeoff, Spectrum Sensing, Channel estimation**

I. Introduction

We are currently in the phase of conceptualizing the requirements of the fifth generation (5G) of mobile wireless systems. One of the major goals is to improve the areal capacity (bits/s/m^2) by a factor of 1000 [2]. A large contribution of this demand is procured by means of an extension to the existing spectrum. Recently, the spectrum beyond 6 GHz, which largely entails the millimeter wave is envisaged as a powerful source of spectrum for 5G systems. However, the millimeter wave technology is still in its nascent stage and along with complex regulatory requirements in this regime, it is surmounted by key challenges like propagation loss, low efficiency of radio frequency components such as power amplifiers, small size of the antenna and link acquisition that need to be addressed [3]. Therefore, to capture a deeper insight of its feasibility in 5G, it is essential to overcome the aforementioned challenges in the forthcoming future.

*A. Kaushik and F. K. Jondral are with Communications Engineering Lab, Karlsruhe Institute of Technology (KIT), Germany. Email:{ankit.kaushik,friedrich.jondral}@kit.edu.

†S.K. Sharma, S. Chatzinotas and B. Ottersten are with SnT - securityandtrust.lu, University of Luxembourg, Luxembourg. Email:{shree.sharma, symeon.chatzinotas, bjorn.ottersten}@uni.lu.

The preliminary analysis of this paper has been presented at CROWNCOM 2015 in Doha, Qatar [1].

This work was partially supported by the National Research Fund, Luxembourg under the CORE projects "SeMIGod" and "SATSENT".

In contrast, the spectrum below 6 GHz, which is appropriate especially for mobile communications, presents an alternative solution. Due to its static allocation, this spectrum is on the verge of depletion. However, it is possible to overcome this scarcity if we manage to utilize this radio spectrum efficiently. In this perspective, Cognitive Radio (CR) is foreseen as one of the potential contenders that addresses the problem of spectrum scarcity. Over the past one and a half decade, this notion has evolved at a tremendous pace right from its origin by Mitola *et al.* in 1999 [4] and consequently, it has acquired certain maturity. However, from a deployment perspective, this technology is still in its preliminary phase. In this view, it is imperative to make substantial efforts that enable the placement of this concept over a hardware platform.

An access to the licensed spectrum is an outcome to the paradigm employed by the Secondary User (SU). Based on the paradigms described in the literature, all CR systems that provide dynamic access to the spectrum fall mainly under three categories, namely, interweave, underlay and overlay systems [5]. In Interweave Systems (ISs), the SUs render an interference-free access to the licensed spectrum by exploiting spectral holes in different domains such as time, frequency, space and polarization, whereas underlay systems enable an interference-tolerant access under which the SUs are allowed to use the licensed spectrum (e.g. Ultra Wide Band) as long as they respect the interference constraints of the Primary Receivers (PRs). Besides that, overlay systems consider participation of higher layers for enabling spectral coexistence between two or more wireless networks. Due to its ease of deployment, IS is mostly preferred not only for performing theoretical analysis but for practical implementation as well. Motivated by these facts, this paper focuses on the performance analysis of the ISs from a deployment perspective.

Motivation and Related Work

Spectrum sensing is an integral part of ISs. At the Secondary Transmitter (ST), sensing is necessary for detecting the presence or absence of a primary signal, thereby protecting the PRs against harmful interference. Sensing at the ST is accomplished by listening to the signal transmitted by the Primary

Transmitter (PT). For detecting a primary signal, several techniques such as energy, matched filtering, cyclostationary and feature-based detection exist [6], [7]. Because of its versatility towards unknown primary signals and its low computational complexity, energy detection has been extensively investigated in the literature [8]–[12]. In energy detection, the decision is accomplished by comparing the power received at the ST to a threshold. In reality, the ST encounters variation in the received power due to existence of thermal noise at the receiver and channel fading. This leads to sensing errors described as misdetection or false alarm, thus, limiting the performance of the IS. In order to determine the performance of the detector, it is essential to characterize the expressions of detection probability and false alarm probability.

In particular, detection probability is critical for the primary system because it protects the PR from the interference induced by the ST. As a result, sustaining a target detection probability is of paramount importance to the ISs [13]. Therefore, the characterization of the detection probability becomes absolutely necessary for the performance analysis of the IS. In this context, Urkowitz [8] introduced a probabilistic model that establishes a fundamental framework for characterizing the sensing errors, however, the characterization accounts only for noise in the system. To encounter the variation caused by channel fading, a frame structure is introduced such that the channel is considered to remain constant over the frame duration, however, upon exceeding the frame duration, the system may witness a different realization of the channel. Based on this frame structure, the performance of the IS has been investigated as *short-term* [14]–[16] and *long-term* [9]–[11] characterization.

The long-term (statistical) characterization is a classical approach that applies a fading model to average out the variation in the received power. Subject to the deployment scenarios[1], different fading models – Rice, Rayleigh, Nakagami-m and Log-normal can be employed [17]. The analytical expressions for the expected detection probability for these fading models are characterized in [9]–[11]. Considering a CR system, this approach has some major drawbacks. Fading models depict a long-term characterization of the system, however, short-term or bursty interference that may lead to outage is ignored, thereby deteriorating the performance of a primary system. Moreover, fading models are specific to the deployment scenario, hence, knowledge of the fading model is necessary when designing a CR system. Apart from that, every fading model contains certain model parameters. As a result, estimation of these parameters at the ST [18], particularly during the initial phase of the deployment, imposes an additional overhead on the secondary system. In practice, due to mobility, most systems are likely to violate stationarity over a long duration. Thus, it becomes challenging to track these model parameters. As a consequence, these drawbacks restrict the applicability of this approach to practical CR systems.

To overcome the aforementioned drawbacks, an alternative approach that considers the short-term characterization has been established [14]–[16] in such a way that the performance can be analyzed for a single frame[2]. In this way, unlike long-term approach, we preclude the variation due to the channel and consider the variation due to noise in the system. Subsequently, this approach does not need to consider the deployment of the fading model and its complexities thereafter. Motivated by these facts, we focus on the short-term approach for performance analysis.

Problem Formulation

Recently, the performance characterization of CR systems in terms of sensing-throughput tradeoff has received significant attention [14], [16], [19], [20]. According to Liang *et al.* [14], the ST assures a reliable detection of a primary signal, thereby sustaining the detection probability above a desired level with an objective of maximizing the throughput at the Secondary Receiver (SR). In this way, the sensing-throughput tradeoff renders a suitable sensing time that achieves a maximum throughput for a given received power. However, to characterize the detection probability and throughput, the system requires the knowledge of interacting channels, namely, a *sensing* channel, an *access* channel and an *interference* channel, cf. Fig. 1[3]. To the best of the authors' knowledge, the baseline models investigated in the literature assume the knowledge of these channels to be available at the ST. However, in practice, this knowledge is not available, thus, needs to be estimated at the ST. As a result, the existing solutions for the IS are considered idealistic for performing analysis, however, they are not suitable for deployment.

Following the previous discussion, it is apparent that the received power, contained in the sensing channel, is crucial for characterizing the detection probability, therefore, is essential for evaluating the detector's performance. The channel, according to the short-term characterization, is regarded as unknown and expected to remain constant over a frame duration, hence, it is reasonable to include received power based estimation for each frame [1]. Inherent to the estimation process, a variation is induced in the detection probability. In this sense, characterizing the performance of a detector with received power estimation remains an open problem. Besides detection probability, false alarm probability largely affects the throughput attained by the secondary system at the SR. Further, the characterization of the false alarm probability requires the knowledge of the noise power. Subject to a given uncertainty [21], this knowledge can be acquired through hardware calibration. In parallel to that, the variation in the detection probability further translates to the variation in the secondary system's throughput. Moreover, the estimation of the access and the interference channels imposes an additional variation on the throughput. Hence, to characterize the performance of the IS in terms of sensing-throughput tradeoff, it is essential to capture these variations in an accurate manner.

[1] These scenarios include urban, suburban and rural, or indoor and outdoor from a different perspective.

[2] By a single frame, we refer to the statistical realizations of the received power, whereas [14]–[16] consider the temporal realizations of the same across several frames. Considering ergodic behaviour of the noise, the performance characterization under these two scenarios are equivalent.

[3] As the interference to the PR is controlled by a regulatory constraint over the detection probability, in this view, the interaction with the PR is excluded in the considered scenario [14].

In order to overcome these difficulties, the following strategy is pursued in this paper. Firstly, we consider received power estimation at the ST that allows us to constrain the detection probability at a desired level. However, with the inclusion of this estimation, the system anticipates: (i) a performance loss in terms of temporal resources used and (ii) variations in the aforementioned performance parameters due to imperfect estimation. A preliminary analysis of this performance loss was carried out in [1], where it was revealed that in low signal to noise ratio regime, imperfect estimation of received power corresponds to large variation in detection probability, hence, causing a severe degradation in the performance of the IS. However, this performance degradation was determined by means of lower and upper bounds. In this work, we consider a more exact analysis, whereby we capture the variation in detection probability by characterizing its distribution function. Using this, we apply new probabilistic constraints on the detection probability that allow IS to operate at low signal to noise ratio regime.

Besides that, we include channel estimation at the SR to acquire the knowledge of the access and interference channels. It is well-known that systems with transmitter information (which includes the filter, pilot symbols, modulation type and time-frequency synchronization) at the receiver acquire channel knowledge by listening to the pilot data sent by the ST [22]–[25]. Other systems, where the receiver possesses either no access to this information or limited by hardware complexity, procure channel knowledge indirectly by estimating a different parameter, for instance, received signal strength or received power, that entails the channel knowledge. Recently, pilot based estimation [26], [27] and received power estimation [28] have been applied to obtain channel knowledge for CR systems. However, the analysis was restricted to underlay systems, where the emphasis was laid on modelling the interference at the PR. In this paper, we extend this concept to the IS, hence, employ pilot based estimation for the access channel and received power based estimation for the sensing and interference channels, cf. Fig. 1. Upon acquiring the knowledge of these channels at the ST, we depict the impact of imperfect channel estimation on the performance of the IS in terms of sensing-throughput tradeoff. Unlike the sensing channel, the access and interference channels have to be estimated at the SR and made available at the ST over a low-rate feedback channel.

Contributions

The major contributions of this paper can be summarized as follows:

- The main goal of the paper is to establish a system model that constitutes the estimation of: (i) sensing channel at the ST, (ii) access and (iii) interference channels at the SR. With the inclusion of estimation, the system witnesses variations in the performance parameters and a certain performance loss. Based on the proposed model, this work investigates these two aspects and characterizes the performance of the IS under realistic conditions.
- To capture the variations induced in the system, we characterize the distribution of performance parameters

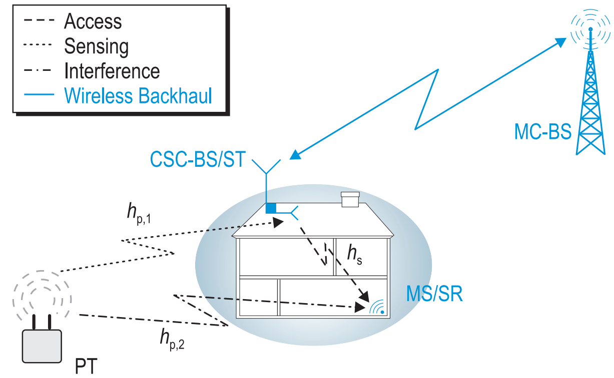

Fig. 1. A cognitive small cell scenario demonstrating: (i) the interweave paradigm, (ii) the associated network elements, which constitute Cognitive Small Cell-Base Station/Secondary Transmitter (CSC-BS/ST), Mobile Station/Secondary Receiver (MS/SR), Macro Cell-Base Station (MC-BS) and Primary Transmitter (PT), (iii) the interacting channels: sensing, access and interference.

  such as detection probability and achievable secondary throughput. More importantly, we utilize the distribution of the detection probability to establish new Primary User (PU) constraints on the detection probability.
- Subject to the new constraints, we establish the expressions of sensing-throughput tradeoff to capture the variations in the performance parameters and evaluate the performance loss in terms of the achievable throughput of the IS.
- Finally, we depict a fundamental tradeoff between estimation time, sensing time and achievable secondary throughput. We exploit this tradeoff to determine a suitable estimation and sensing time that depicts the maximum achievable performance of the IS.

Organization

The subsequent sections of the paper are organized as follows: Section II describes the system model that includes the deployment scenario, the signal model and the performance characterization for the ideal scenario for the IS. Section III presents the proposed model that incorporates channel estimation. Section IV characterizes the distribution of the performance parameters and establishes the sensing-throughput tradeoff subject to average and outage constraints. Section V analyzes the numerical results based on the obtained expressions. Finally, Section VI concludes the paper. Table I lists the definitions of acronyms and important mathematical notations used throughput the paper.

II. System Model

Deployment Scenario

Cognitive Small Cell (CSC), a CR application, characterizes a small cell deployment that fulfills the spectral requirements for Mobile Stations (MSs) operating indoor, cf. Fig. 1. For the disposition of the CSC in the network, the following key elements are essential: a CSC-Base Station (CSC-BS), a Macro Cell-Base Station (MC-BS) and MS, cf. Fig. 1. MSs are the indoor devices served by the CSC-BS over an access channel (h_s). Furthermore, the MC-BS is connected

TABLE I
DEFINITIONS OF ACRONYMS AND NOTATIONS USED

Acronyms and Notations	Definitions
AC, OC	Average Constraint, Outage Constraint
CR	Cognitive Radio
CSC, CSC-BS, MC-BS, MS	Cognitive Small Cell, Cognitive Small Cell-Base Station, Macro Cell-Base Station, Mobile Station
IM, EM	Ideal Model, Estimation Model
IS	Interweave System
PU - PT, PR	Primary User - Primary Transmitter, Primary Receiver
SU - ST, SR	Secondary User - Secondary Transmitter, Secondary Receiver
$\mathcal{H}_1, \mathcal{H}_0$	Signal plus noise hypothesis, noise only hypothesis
f_s	Sampling frequency
$\tau_\text{est}, \tau_\text{sen}$	Estimation time, sensing time interval
T	Frame duration
$\text{P}_\text{d}, \text{P}_\text{fa}$	Probability of detection, false alarm probability
$\bar{\text{P}}_\text{d}$	Target detection probability
κ	Outage Constraint over detection probability
$h_\text{p,1}, h_\text{p,2}, h_\text{s}$	Channel coefficient for the link PT-ST, PT-SR, ST-SR
$\gamma_\text{p,1}, \gamma_\text{p,2}, \gamma_\text{s}$	Signal to noise ratio for the link PT-ST, PT-SR, ST-SR
R_s	Throughput at SR
C_0, C_1	Shanon capacity at SR without and with interference from PT
μ	Threshold for the energy detector
$F_{(\cdot)}$	Cumulative distribution function of random variable $(\cdot)$
$f_{(\cdot)}$	Probability density function of random variable $(\cdot)$
$\hat{(\cdot)}$	Estimated value of $(\cdot)$
$\tilde{(\cdot)}$	Suitable value of the parameter $(\cdot)$ that achieves maximum performance
$\mathbb{E}_{(\cdot)}$	Expectation with respect to $(\cdot)$
$\mathbb{P}$	Probability measure
$\mathbf{T}(\cdot)$	Test statistics
σ_x^2, σ_w^2	Signal variance at PT, noise variance at ST and SR
N_s	Number of pilot symbols used for pilot based estimation at the SR for h_s
$N_\text{p,2}$	Number of samples used for received power estimation at the SR for $h_\text{p,2}$

to several CSC-BSs over a wireless backhaul[4]. Moreover, the transmissions from the PT can be listened by the CSC-BS and the MS over sensing ($h_\text{p,1}$) and interference channel ($h_\text{p,2}$), respectively. Considering the fact that the IS is employed at the CSC-BS, the CSC-BS and the MS represent ST and SR, respectively. A hardware prototype of the CSC-BS operating as IS was presented in [29]. For simplification, a PU constraint based on false alarm probability was considered in [29]. With the purpose of improving system's reliability, we extend the analysis to employ a PU constraint on the detection probability.

As a follow-on from the ideal model depicted in [14], we consider a slotted medium access for the IS, where the time axis is segmented into frames of length T, according to which, the ST employs periodic sensing. Hence, each frame consists of a sensing slot τ_sen and the remaining duration $T - \tau_\text{sen}$ is utilized for data transmission. For small T relative to the PU's expected ON/OFF period, the requirement of the ST to be in alignment to PUs' medium access can be relaxed [30]–[32].

[4] A wireless backhaul is a point-to-point wireless link between the CSC-BS and MC-BS that relays the traffic generated from the CSC to the core network.

Signal model

Subject to the underlying hypothesis that illustrates the presence ($\mathcal{H}_1$) or absence ($\mathcal{H}_0$) of a primary signal, the discrete and real signal received at the ST is given by

$$y_\text{ST}[n] = \begin{cases} h_\text{p,1} \cdot x_\text{PT}[n] + w[n] & : \mathcal{H}_1 \\ w[n] & : \mathcal{H}_0 \end{cases}, \quad (1)$$

where $x_\text{PT}[n]$ corresponds to a discrete and real sample transmitted by the PT, $|h_\text{p,1}|^2$ represents the power gain of the sensing channel for a given frame and $w[n]$ is additive white Gaussian noise at the ST. In [14], the primary signal $x_\text{PT}[n]$ has been modelled as: (i) phase shift keying modulated signal, or (ii) Gaussian signal. The signals that are prone to high inter-symbol interference or entail precoding can be modelled as Gaussian signals. For this paper, we focus our analysis on the latter case. As a result, mean and variance for the signal and the noise are determined as $\mathbb{E}[x_\text{PT}[n]] = 0$, $\mathbb{E}[w[n]] = 0$, $\mathbb{E}\left[|x_\text{PT}[n]|^2\right] = \sigma_x^2$ and $\mathbb{E}\left[|w[n]|^2\right] = \sigma_w^2$. The channel $h_\text{p,1}$ is considered to be independent of $x_\text{PT}[n]$ and $w[n]$, thus, y_ST is also an independent and identically distributed (i.i.d.) random process.

Similar to (1), during data transmission, the discrete and real received signal at the SR conditioned on the detection probability (P_d) and false alarm probability (P_fa) is given by

$$y_\text{SR}[n] = \begin{cases} h_\text{s} \cdot x_\text{ST}[n] + h_\text{p,2} \cdot x_\text{PT}[n] + w[n] & : 1 - \text{P}_\text{d} \\ h_\text{s} \cdot x_\text{ST}[n] + w[n] & : 1 - \text{P}_\text{fa} \end{cases}, \quad (2)$$

where $x_\text{ST}[n]$ corresponds to discrete and real sample transmitted by the ST. Further, $|h_\text{s}|^2$ and $|h_\text{p,2}|^2$ represent the power gains for access and interference channels, cf. Fig. 1.

Sensing

Following the frame structure, ST performs sensing for a duration of τ_sen. The test statistics $\text{T}(\mathbf{y})$ at the ST is evaluated as

$$\text{T}(\mathbf{y}) = \frac{1}{\tau_\text{sen} f_\text{s}} \sum_{n=1}^{\tau_\text{sen} f_\text{s}} |y_\text{ST}[n]|^2 \underset{\mathcal{H}_0}{\overset{\mathcal{H}_1}{\gtrless}} \mu, \quad (3)$$

where μ is the decision threshold and $\mathbf{y}$ is a vector with $\tau_\text{sen} f_\text{s}$ samples. $\text{T}(\mathbf{y})$ represents a random variable, whereby the characterization of the distribution function depends on the underlying hypothesis. Corresponding to $\mathcal{H}_0$ and $\mathcal{H}_1$, $\text{T}(\mathbf{y})$ follows a central chi-squared ($\mathcal{X}^2$) distribution [33]. As a result, the detection probability (P_d) and the false alarm probability (P_fa) corresponding to (3) are determined as [21]

$$\text{P}_\text{d}(\mu, \tau_\text{sen}, P_\text{Rx,ST}) = \Gamma\left(\frac{\tau_\text{sen} f_\text{s}}{2}, \frac{\tau_\text{sen} f_\text{s} \mu}{2 P_\text{Rx,ST}}\right), \quad (4)$$

$$\text{P}_\text{fa}(\mu, \tau_\text{sen}) = \Gamma\left(\frac{\tau_\text{sen} f_\text{s}}{2}, \frac{\tau_\text{sen} f_\text{s} \mu}{2 \sigma_w^2}\right), \quad (5)$$

where $P_\text{Rx,ST}$ is the power received over the sensing channel and $\Gamma(\cdot,\cdot)$ represents a regularized upper Gamma function [34].

Sensing-Throughput tradeoff

Following the characterization of $\mathrm{P_{fa}}$ and $\mathrm{P_d}$, Liang *et. al.* [14] established a tradeoff between the sensing time and secondary throughput (R_s) subject to a target detection probability ($\bar{\mathrm{P}}_\mathrm{d}$). This tradeoff is represented as

$$R_\mathrm{s}(\tilde{\tau}_\mathrm{sen}) = \max_{\tau_\mathrm{sen}} R_\mathrm{s}(\tau_\mathrm{sen}) = \frac{T-\tau_\mathrm{sen}}{T}\Big[\mathrm{C_0}(1-\mathrm{P_{fa}})\mathbb{P}(\mathcal{H}_0) + \mathrm{C_1}(1-\mathrm{P_d})\mathbb{P}(\mathcal{H}_1)\Big], \quad (6)$$

$$\text{s.t. } \mathrm{P_d} \geq \bar{\mathrm{P}}_\mathrm{d}, \quad (7)$$

$$\text{where } \mathrm{C_0} = \log_2\left(1 + |h_\mathrm{s}|^2 \frac{P_\mathrm{Tx,ST}}{\sigma_w^2}\right) = \log_2(1+\gamma_\mathrm{s}) \quad (8)$$

$$\text{and } \mathrm{C_1} = \log_2\left(1 + \frac{|h_\mathrm{s}|^2 P_\mathrm{Tx,ST}}{|h_\mathrm{p,2}|^2 P_\mathrm{Tx,PT} + \sigma_w^2}\right) = \log_2\left(1 + \frac{|h_\mathrm{s}|^2 P_\mathrm{Tx,ST}}{P_\mathrm{Rx,SR}}\right) = \log_2\left(1 + \frac{\gamma_\mathrm{s}}{\gamma_\mathrm{p,2}+1}\right), \quad (9)$$

where $\mathbb{P}(\mathcal{H}_0)$ and $\mathbb{P}(\mathcal{H}_1)$ are the probabilities of occurrence for the respective hypothesis, whereas $\gamma_\mathrm{p,2}$ and γ_s correspond to signal to noise ratio for the links PT-SR and ST-SR, respectively. Moreover, $P_\mathrm{Tx,ST}$ and $P_\mathrm{Tx,PT}$ represent the transmit power at the PT and the ST, whereas $P_\mathrm{Rx,SR}$ corresponds to the received power at the SR. In other words, using (6), the ST determines a suitable sensing time $\tau_\mathrm{sen} = \tilde{\tau}_\mathrm{sen}$, such that the throughput is maximized subject to a target detection probability, cf. (7). From the deployment perspective, the tradeoff depicted above has the following fundamental issues:

- Without the knowledge of the received power (sensing channel), it is not feasible to characterize $\mathrm{P_d}$. This leaves the characterization of the throughput (6) impossible and the constraint defined in (7) inappropriate.
- Moreover, the knowledge of the interacting channels is required at the ST, cf. (8) and (9) for characterizing the throughput in terms of $\mathrm{C_0}$ and $\mathrm{C_1}$ at the SR.

Taking into account these issues, it is not sensible to employ the performance analysis depicted by the ideal model for hardware implementation. In the subsequent section, we propose an estimation model that addresses these issues, thereby including the estimation of the sensing channel at the ST, and interference and access channels at the SR. Based on the proposed model, we then investigate the performance of the IS in terms of the sensing-throughput tradeoff.

III. Proposed Model

The inclusion of estimation of the interacting channels causes variations in the parameters $\mathrm{P_d}$, $\mathrm{C_0}$ and $\mathrm{C_1}$. Unless characterized, these variations may seriously degrade the performance of the hardware deployed. In this view, we include the estimation of the interacting channels in the system model, thereby characterizing the variations in $\mathrm{P_d}$, $\mathrm{C_0}$ and $\mathrm{C_1}$ by means of their their distribution functions $F_{\mathrm{P_d}}$, $F_{\mathrm{C_0}}$ and $F_{\mathrm{C_1}}$. By utilizing these expressions, we finally obtain a characterization of sensing-throughput tradeoff. To include channel estimation, we propose a frame structure that constitutes estimation τ_est, sensing τ_sen and data transmission $T-(\tau_\mathrm{est}+\tau_\mathrm{sen})$, where $\tau_\mathrm{est}, \tau_\mathrm{sen}$ correspond to time intervals and $\tau_\mathrm{est}+\tau_\mathrm{sen} < T$, cf. Fig. 2. In practice, the estimated values of the interacting channels are required for determining the suitable sensing time, hence, the sequence depicted in Fig. 2, whereby estimation followed by sensing is reasonable for the hardware deployment. In this regard, a low-rate feedback channel from the SR to the ST is required for the proposed model.

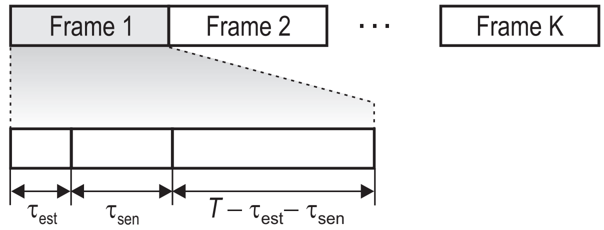

Fig. 2. Frame structure of interweave system with received power estimation.

Besides that, particularly for the sensing channel, the samples used for estimation can be combined with the samples acquired for sensing ($\tau_\mathrm{sen}^* = \tau_\mathrm{est} + \tau_\mathrm{sen}$), thereby improving the performance of the detector at the ST. As τ_sen^* is dependent on $P_\mathrm{Rx,ST}$ or the state of $h_\mathrm{p,1}$ in particular, under this situation, τ_sen^* is lower bounded by τ_est, consequently translating $F_{\mathrm{P_d}}$ from a continuous function to a piecewise continuous function, thereby complicating the analytical tractability of $F_{\mathrm{P_d}}$. Hence, to simplify the analysis, in this work, we consider estimation and sensing as disjoint events in time. In this regard, the derived expressions based on our proposed model represents a lower performance bound. Next, in the following subsections, we present the estimation of the interacting channels.

Estimation of sensing channel ($h_{p,1}$)

Following the previous discussions, the ST acquires the knowledge of $h_\mathrm{p,1}$ by estimating its received power. The estimated received power is required for the characterization of $\mathrm{P_d}$, thereby evaluating the detector performance.

Under $\mathcal{H}_1$, the received power estimated during the estimation phase at the ST is given as [8]

$$\hat{P}_\mathrm{Rx,ST} = \frac{1}{\tau_\mathrm{est} f_\mathrm{s}} \sum_{n=1}^{\tau_\mathrm{est} f_\mathrm{s}} |y_\mathrm{ST}[n]|^2. \quad (10)$$

$\hat{P}_\mathrm{Rx,ST}$ determined in (10) using $\tau_\mathrm{est} f_\mathrm{s}$ samples follows a central chi-squared distribution $\mathcal{X}^2$ [33]. The cumulative distribution function of $\hat{P}_\mathrm{Rx,ST}$ is given by

$$F_{\hat{P}_\mathrm{Rx,ST}}(x) = \Gamma\left(\frac{\tau_\mathrm{est} f_\mathrm{s}}{2}, \frac{\tau_\mathrm{est} f_\mathrm{s} x}{2 P_\mathrm{Rx,ST}}\right). \quad (11)$$

Estimation of access channel (h_s)

The signal received from the ST undergoes matched filtering and demodulation at the SR, hence, it is reasonable to employ pilot based estimation for h_s. Unlike received power estimation, pilot based estimation renders a direct estimation of the channel. Now, to accomplish pilot based estimation, the SR aligns itself to pilot symbols transmitted by the ST. Under $\mathcal{H}_0$, the discrete and real pilot symbols at the output of the demodulator is given by [24]

$$p[n] = \sqrt{E_\mathrm{s}} h_\mathrm{s} + w[n], \quad (12)$$

where E_s denotes the pilot energy. Without loss of generality, the pilot symbols are considered to be +1. The maximum likelihood estimate, representing a sample average of N_s pilot symbols, is given by [23]

$$h_s = \hat{h}_s + \underbrace{\frac{\sum_n^{N_s} p[n]}{2N_s}}_{\epsilon}, \tag{13}$$

where ϵ denotes the estimation error. The estimate $\hat{h}_s$ is unbiased, efficient and achieves a Cramer-Rao bound with equality, with variance $\mathbb{E}\left[|h_s - \hat{h}_s|^2\right] = \sigma_w^2/(2N_s)$ [24]. Consequently, $\hat{h}_s$ conditioned on h_s follows a Gaussian distribution.

$$\hat{h}_s|h_s \sim \mathcal{N}\left(h_s, \frac{\sigma_w^2}{2N_s}\right). \tag{14}$$

As a result, the power gain $|\hat{h}_s|^2$ follows a non-central chi-squared ($\mathcal{X}_1^2$) distribution with 1 degree of freedom and non-centrality parameter $\lambda = \frac{2N_s|h_s|^2}{\sigma_w^2}$.

Estimation of interference channel ($h_{p,2}$)

In addition, analog to sensing channel, the SR performs received power estimation by listening to the transmission from the PT. The knowledge of $h_{p,2}$ is required to characterize interference from the PT. Under $\mathcal{H}_1$, the discrete signal model at the SR is given as

$$y_{SR}[n] = h_{p,2} \cdot x_{PT}[n] + w[n]. \tag{15}$$

The received power at the SR from the PT given by

$$\hat{P}_{Rx,SR} = \frac{1}{N_{p,2}} \sum_{n=1}^{N_{p,2}} |y_{SR}[n]|^2, \tag{16}$$

follows a $\mathcal{X}^2$ distribution, where $N_{p,2}$ corresponds to the number of samples used for estimation.

Assumptions and Approximations

To simplify the analysis and sustain analytical tractability for the proposed model, several assumptions considered in the paper are summarized as follows:

- We consider that all transmitted signals are subjected to distance dependent path loss and small scale fading gain. With no loss of generality, we consider that the channel gains include distance dependent path loss and small scale gain. Moreover, the coherence time for the channel gain is considered to be greater than the frame duration[5].
- To ensure mathematical tractability of the proposed model, we consider disjoint sets of samples for estimation and sensing for a certain frame. However, in practice, it is possible to utilize the samples used in the estimation phase for sensing purpose as well, which leads to an improvement in the detector's performance in terms of the number of samples utilized for sensing.
- We assume perfect knowledge of the noise power in the system, however, the uncertainty in noise power can be captured as a bounded interval [21]. Inserting this interval in the derived expressions, cf. Section IV, the performance of the IS can be expressed in terms of the upper and the lower bounds.
- For all degrees of freedom, $\mathcal{X}_1^2$ distribution can be approximated as Gamma distribution [35]. The parameters of the Gamma distribution are obtained by matching the first two central moments to those of $\mathcal{X}_1^2$.
- Analog to [14], [16], [19], [20], the proposed model stipulates the knowledge of the underlying hypothesis at the ST and the SR. With the knowledge of occurrence probabilities $\mathbb{P}(\mathcal{H}_0)$ and $\mathbb{P}(\mathcal{H}_1)$ and subsequently applying PU traffic models proposed in [30]–[32], it is possible to acquire this knowledge with high probability.
- Considering a realistic situation, it is possible that SR might not accomplish estimation in each frame, under such circumstances, the ST utilizes the previous estimation value for the sensing-throughput analysis.

[5]In the scenarios where the coherence time exceeds the frame duration, in such cases our characterization depicts a lower performance bound.

IV. Theoretical Analysis

At this stage, it is evident that the variation due to imperfect channel estimation translates to the variations of the performance parameters P_d, C_0 and C_1, which are fundamental to sensing-throughput tradeoff. Below, we capture these variations by characterizing their cumulative distribution functions F_{P_d}, F_{C_0} and F_{C_1}, respectively.

Lemma 1: The cumulative distribution function of P_d is characterized as

$$F_{P_d}(x) = 1 - \Gamma\left(\frac{\tau_{est} f_s}{2}, \frac{\tau_{est} f_s \tau_{sen} f_s \mu}{4 P_{Rx,ST} \Gamma^{-1}\left(\frac{\tau_{sen}}{2}, x\right)}\right), \tag{17}$$

where $\Gamma^{-1}(\cdot,\cdot)$ is inverse function of regularized upper Gamma function [34].

Proof: The cumulative distribution function of P_d is defined as

$$F_{P_d}(x) = \mathbb{P}(P_d(\mu, \tau_{sen}, \hat{P}_{Rx,ST}) \le x). \tag{18}$$

Using (4)

$$= \mathbb{P}\left(\Gamma\left(\frac{\tau_{sen} f_s}{2}, \frac{\tau_{est} f_s \mu}{2\hat{P}_{Rx,ST}}\right) \le x\right), \tag{19}$$

$$= 1 - \mathbb{P}\left(\hat{P}_{Rx,ST} \le \frac{\mu \tau_{sen} f_s}{2\Gamma^{-1}\left(\frac{\tau_{sen} f_s}{2}, x\right)}\right). \tag{20}$$

Replacing the cumulative distribution function of $\hat{P}_{Rx,ST}$ in (20), we obtain an expression of F_{P_d}. ∎

Lemma 2: The cumulative distribution function of C_0 is defined as

$$F_{C_0}(x) = \int_0^x f_{C_0}(t) dt, \tag{21}$$

where

$$f_{C_0}(x) = 2^x \ln 2 \frac{(2^x - 1)^{a_1 - 1}}{\Gamma(a_1) b_1^{a_1}} \exp\left(-\frac{2^x - 1}{b_1}\right), \tag{22}$$

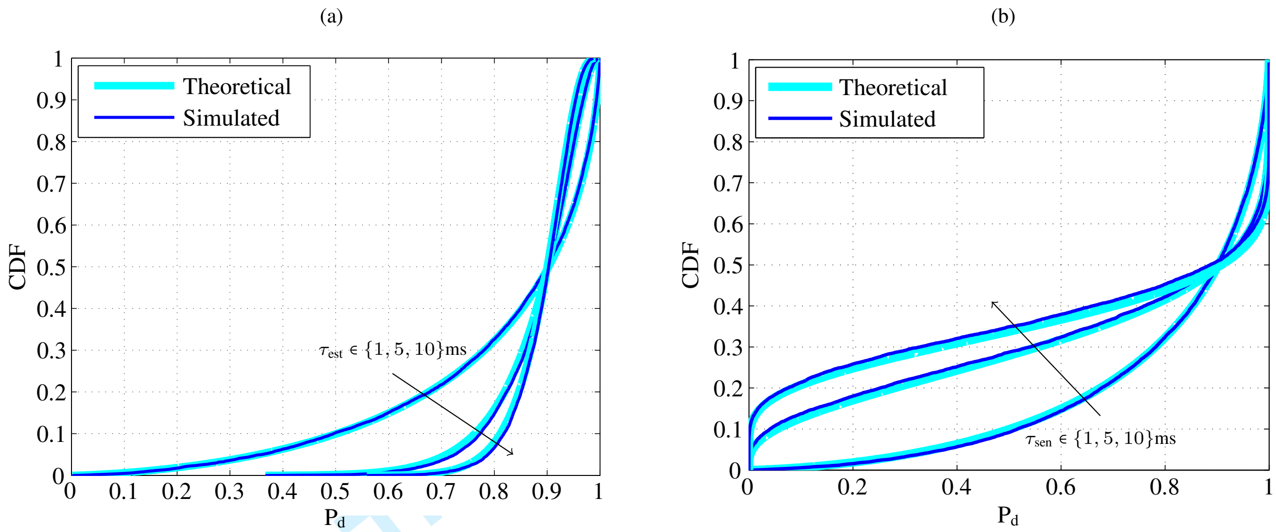

Fig. 3. CDF of $\mathrm{P_d}$ for different τ_{est} and τ_{sen}. (a) $\tau_{\text{est}} \in \{1, 5, 10\}$ms and $\tau_{\text{sen}} = 1$ ms, (b) $\tau_{\text{est}} = 1$ ms and $\tau_{\text{sen}} \in \{1, 5, 10\}$ms.

and

$$a_1 = \frac{\left(\frac{\sigma_w^4}{2N_s P_{\text{Tx,ST}}} + |h_s|^2\right)^2}{\frac{\sigma_w^4}{2N_s P_{\text{Tx,ST}}}\left(2\frac{\sigma_w^4}{2N_s P_{\text{Tx,ST}}} + 4|h_s|^2\right)},$$
$$b_1 = \frac{\frac{\sigma_w^4}{2N_s P_{\text{Tx,ST}}}\left(2\frac{\sigma_w^4}{2N_s P_{\text{Tx,ST}}} + 4|h_s|^2\right)}{\left(\frac{\sigma_w^4}{2N_s P_{\text{Tx,ST}}} + |h_s|^2\right)}. \tag{23}$$

Proof: Following the probability density function (pdf) of $|\hat{h}_s|^2$ in (14), the pdf $|\hat{h}_s|^2 \frac{P_{\text{Tx,ST}}}{\sigma_w^2}$ is given by

$$f_{\frac{|\hat{h}_s|^2 P_{\text{Tx,ST}}}{\sigma_w^2}}(x) = \frac{2N_s P_{\text{Tx,ST}}}{\sigma_w^4}\frac{1}{2}\exp\left[-\frac{1}{2}\left(x\frac{\sigma_w^4}{2N_s P_{\text{Tx,ST}}} + \lambda\right)\right] \times \left(\frac{x}{\lambda}\frac{\sigma_w^4}{2N_s P_{\text{Tx,ST}}}\right)^{\frac{N_s}{4}-\frac{1}{2}} I_{\frac{N_s}{2}-1}\left(\sqrt{\lambda x \frac{\sigma_w^4}{2N_s P_{\text{Tx,ST}}}}\right),$$

where $I_{(\cdot)}(\cdot)$ represents the modified Bessel function of first kind [34]. Approximating $\mathcal{X}_1^2(\cdot,\cdot)$ with Gamma distribution $\Gamma(a_1, b_1)$ [35] gives

$$f_{\frac{|\hat{h}_s|^2 P_{\text{Tx,ST}}}{\sigma_w^2}} \approx \frac{1}{\Gamma(a_1)}\frac{x^{a_1-1}}{b_1^{a_1}}\exp\left(-\frac{x}{b_1}\right), \tag{24}$$

where the parameters a_1 and b_1 in (24) are determined by comparing the first two central moments of the two distributions. Finally, by substituting the expression of $\mathrm{C_0}$ in (8) yields (22). ■

Lemma 3: The cumulative distribution function of $\mathrm{C_1}$ is given by

$$F_{\mathrm{C_1}}(x) = \int_0^x f_{\mathrm{C_1}}(t)dt, \tag{25}$$

where

$$f_{\mathrm{C_1}}(x) = 2^x \ln 2 \frac{(2^x-1)^{a_1-1}\Gamma(a_1+a_2)}{\Gamma(a_1)\Gamma(a_2)b_1^{a_1}b_2^{a_2}}\left(\frac{1}{b_2} + \frac{2^x-1}{b_1}\right), \tag{26}$$

and

$$a_2 = \frac{N_{\text{p},2}}{2} \text{ and } b_2 = \frac{2P_{\text{Rx,ST}}}{\sigma_w^2 N_{\text{p},2}}, \tag{27}$$

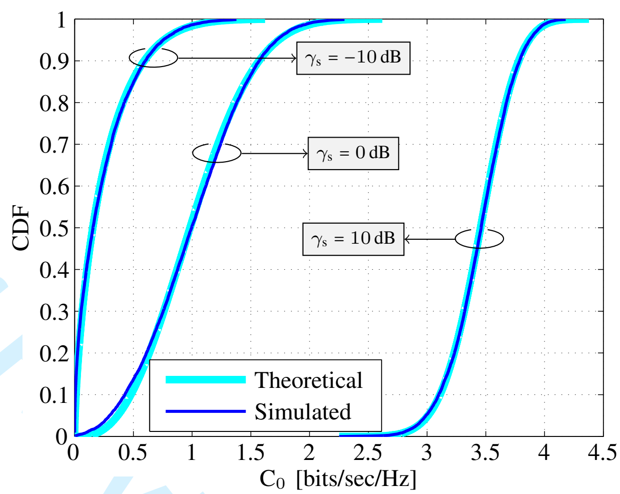

Fig. 4. CDF of $\mathrm{C_0}$ for different values of $\gamma_s \in \{-10, 0, 10\}$dB.

where a_1 and b_1 are defined in (23).

Proof: For simplification, we break down the expression $\left(\frac{|\hat{h}_s|^2 P_{\text{Tx,ST}}}{\hat{P}_{\text{Rx,SR}}}\right)$ in (9), as $E_1 = \left(\frac{|\hat{h}_s|^2 P_{\text{Tx,ST}}}{\sigma_w^2}\right)$ and $E_2 = \left(\frac{\hat{P}_{\text{Rx,SR}}}{\sigma_w^2}\right)$, where $\mathrm{C_1} = \log_2\left(1 + \frac{E_1}{E_2}\right)$. The pdf of the expression E_1 is determined in (24).

Following the characterization $\hat{P}_{\text{Rx,SR}}$ in (16), the pdf of E_2 is determined as

$$f_{\frac{\hat{P}_{\text{Rx,SR}}}{\sigma_w^2}} = \frac{N_{\text{p},2}\sigma_w^2}{P_{\text{Rx,ST}}}\frac{1}{2^{\frac{N_{\text{p},2}}{2}}\Gamma\left(\frac{N_{\text{p},2}}{2}\right)}\left(x\frac{N_{\text{p},2}\sigma_w^2}{P_{\text{Rx,ST}}}\right)^{\frac{N_{\text{p},2}}{2}-1} \times \exp\left(-x\frac{N_{\text{p},2}\sigma_w^2}{2P_{\text{Rx,ST}}}\right). \tag{28}$$

Using the characterizations of pdfs $f_{\frac{|\hat{h}_s|^2 P_{\text{Tx,ST}}}{\sigma_w^2}}$ and $f_{\frac{\hat{P}_{\text{Rx,SR}}}{\sigma_w^2}}$, we apply Mellin transform [36] to determine the pdf of $\frac{E_1}{E_2}$ as

$$f_{\frac{|\hat{h}_s|^2 P_{\text{Tx,ST}}}{\sigma_w^2} / \frac{\hat{P}_{\text{Rx,SR}}}{\sigma_w^2}}(x) = \frac{x^{a_1-1}\Gamma(a_1+a_2)}{\Gamma(a_1)\Gamma(a_2)b_1^{a_1}b_2^{a_2}}\left(\frac{1}{b_2} + \frac{x}{b_1}\right). \tag{29}$$

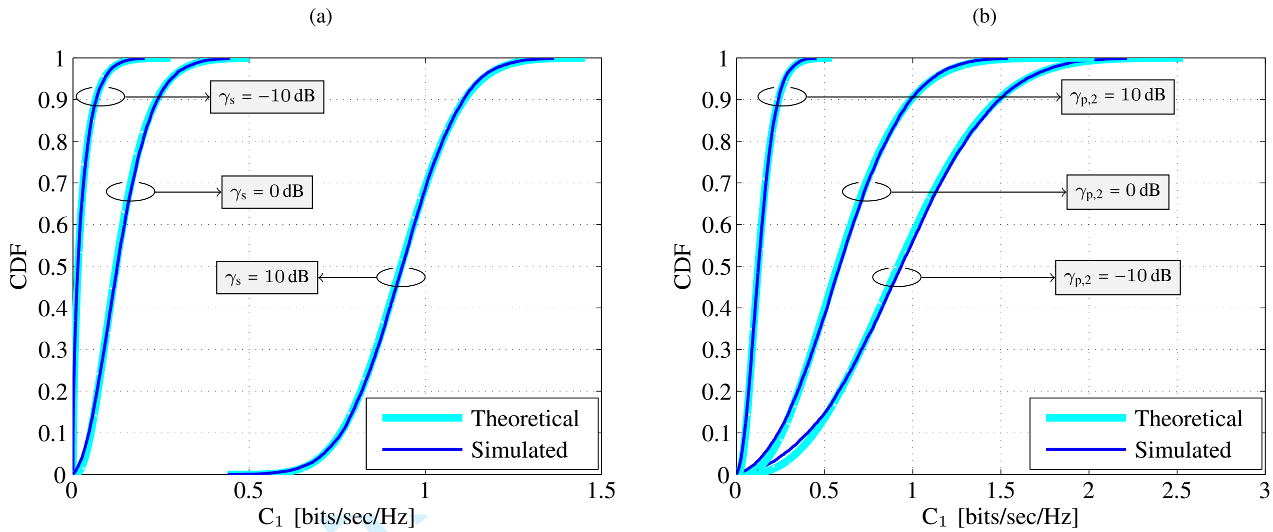

Fig. 5. CDF of C_1 for different γ_s and $\gamma_{p,2}$. (a) $\gamma_s \in \{-10, 0, 10\}$dB and $\gamma_{p,2} = 10\,$dB, (b) $\gamma_s = 0\,$dB and $\gamma_{p,2} \in \{-10, 0, 10\}$dB.

Finally, substituting the expression $\frac{E_1}{E_2}$ in C_1 yields (26). ■

The theoretical expressions of the distribution functions depicted in Lemma 1, Lemma 2 and Lemma 3 are validated by means of simulations in Fig. 3, Fig. 4 and Fig. 5, respectively, with different choices of system parameters, these include $\tau_{\text{est}} \in \{1, 5, 10\}$ms, $\tau_{\text{sen}} = \{1, 5, 10\}$ms, $\gamma_s \in \{-10, 0, 10\}$dB and $\gamma_{p,2} \in \{-10, 0, 10\}$dB.

Sensing-throughput tradeoff

Here, we establish sensing-throughput tradeoff for the estimation model that includes estimation time and incorporates variations in the performance parameter. Most importantly, by capturing these variations, we establish two new PU constraints at the PR, namely, an average constraint and an outage constraint on the detection probability. These constraints restrain the harmful interference at the PR. Based on these constraints and a certain choice of estimation time τ_{est}, we characterize the sensing-throughput tradeoff for the IS.

Theorem 1: Subject to an average constraint on P_d at the PR, the sensing-throughput tradeoff is given by

$$
\begin{aligned}
R_s(\tilde{\tau}_{\text{sen}}) &= \max_{\tau_{\text{sen}}} \mathbb{E}_{P_d, C_0, C_1}\left[R_s(\tau_{\text{sen}})\right], \\
&= \frac{T - \tau_{\text{sen}} - \tau_{\text{est}}}{T}\Big[\mathbb{E}_{C_0}\left[C_0\right](1 - P_{fa})\mathbb{P}(\mathcal{H}_0) \\
&\quad + \mathbb{E}_{C_1}\left[C_1\right](1 - \mathbb{E}_{P_d}\left[P_d\right])\mathbb{P}(\mathcal{H}_1)\Big], \qquad (30)\\
&\text{s.t. } \mathbb{E}_{P_d}\left[P_d\right] \le \bar{P}_d, \qquad (31)
\end{aligned}
$$

where $\mathbb{E}_{P_d}[\cdot]$ represents the expectation with respect to P_d, $\mathbb{E}_{P_d, C_0, C_1}[\cdot]$ denotes the expectation with respect to P_d, C_0 and C_1. Unlike (7), $\bar{P}_d$ in (30) represents the constraint on expected detection probability.

Proof: The proof of Theorem 1 is included in the proof of Theorem 2. ■

Theorem 2: Subject to an outage constraint on P_d at the PR, the sensing-throughput tradeoff is given by

$$
\begin{aligned}
R_s(\tilde{\tau}_{\text{sen}}) &= \max_{\tau_{\text{sen}}} \mathbb{E}_{P_d, C_0, C_1}\left[R_s(\tau_{\text{sen}})\right], \\
&= \frac{T - \tau_{\text{sen}} - \tau_{\text{est}}}{T}\Big[\mathbb{E}_{C_0}\left[C_0\right](1 - P_{fa})\mathbb{P}(\mathcal{H}_0) \\
&\quad + \mathbb{E}_{C_1}\left[C_1\right](1 - \mathbb{E}_{P_d}\left[P_d\right])\mathbb{P}(\mathcal{H}_1)\Big], \qquad (32)\\
&\text{s.t. } \mathbb{P}(P_d \le \bar{P}_d) \le \kappa, \qquad (33)
\end{aligned}
$$

where κ represents the outage constraint.

Proof: In order to solve the constrained optimization problems illustrated in Theorem 1 and Theorem 2, the following approach is considered. As a first step, an underlying constraint is employed to determine μ as a function of the τ_{sen} and τ_{est}.

For the average constraint, the expression $\mathbb{E}_{P_d}[P_d]$ in (31) did not lead to a closed form expression, consequently, no analytical expression of μ is obtained. In this context, we procure μ for the average constraint numerically from (31).

Next, we determine μ based on the outage constraint. This is accomplished by combining the expression of F_{P_d} in (17) with the outage constraint (33)

$$
P(P_d \le \bar{P}_d) = F_{P_d}(\bar{P}_d) \le \kappa. \qquad (34)
$$

Rearranging (34) gives

$$
\mu \ge \frac{4 P_{\text{Rx,ST}} \Gamma^{-1}\left(1 - \kappa, \frac{\tau_{\text{est}} f_s}{2}\right) \Gamma^{-1}\left(1 - \bar{P}_d, \frac{\tau_{\text{sen}} f_s}{2}\right)}{\tau_{\text{est}} \tau_{\text{sen}} (f_s)^2}. \qquad (35)
$$

Upon replacing the respective thresholds in P_d and P_{fa} and evaluating the expectation over P_d, C_0 and C_1 using the distribution functions characterized in Lemma 1, Lemma 2 and Lemma 3, we determine the expected throughput as a function of sensing and estimation time. ■

As a consequence, for a certain estimation time, the sensing-throughput tradeoff that depicts the variation of expected throughput against the sensing time is established based on the average and outage constraints. In contrast to the ideal model, the sensing-throughput tradeoff substantiated by the

TABLE II
PARAMETERS FOR NUMERICAL ANALYSIS

Parameter	Value
f_s	1 MHz
$h_{p,1}, h_{p,2}$	−100 dB
h_s	−80 dB
T	100 ms
$\bar{P}_d$	0.9,
κ	0.05
σ_w^2	−100 dBm
$\gamma_{p,1}$	−10 dB
$\gamma_{p,2}$	−10 dB
γ_s	10 dB
$\sigma_x^2 = P_{Tx,PT}$	−10 dBm
$P_{Tx,ST}$	−10 dBm
$\mathbb{P}(\mathcal{H}_1) = 1 - \mathbb{P}(\mathcal{H}_0)$	0.2
τ_{est}	5 ms
N_s	10
$N_{p,2}$	1000

estimation model, which incorporates the channel knowledge is qualified for characterizing the performance of IS.

Corollary 1: Herein, based on the estimation model, we establish a fundamental relation between estimation time (regulates the variation in the detection probability according to the PU constraint), sensing time (represents the detector performance) and achievable throughput, this relationship is characterized as estimation-sensing-throughput tradeoff. Based on this tradeoff, we determine the suitable estimation $\tau_{est} = \tilde{\tau}_{est}$ and sensing time $\tau_{sen} = \tilde{\tau}_{sen}$ that attains a maximum achievable throughput $R_s(\tilde{\tau}_{est}, \tilde{\tau}_{sen})$ for the IS.

V. NUMERICAL RESULTS

Here, we investigate the performance of the IS based on the proposed model. To accomplish this: (i) we perform simulations to validate the expressions obtained, (ii) we analyze the performance loss incurred due to the estimation. In this regard, we consider the ideal model for benchmarking and evaluating the performance loss, (iii) we establish mathematical justification to the considered approximations. Although, the expressions derived using our sensing-throughput analysis are general and applicable to all CR systems, the parameters are selected in such a way that they closely relate to the deployment scenario described in Fig. 1. Unless stated explicitly, the choice of the parameters given in Table II is considered for the analysis.

Firstly, we analyze the performance of the IS in terms of sensing-throughput tradeoff corresponding to the ideal model (IM) and estimation model (EM) by fixing $\tau_{est} = 5$ ms, cf. Fig. 6. In contrast to constraint on P_d for the ideal model, we employ average constraint (EM-AC) and outage constraint (EM-OC) for the proposed estimation model. With the inclusion of received power estimation in the frame structure, the ST procures no throughput at the SR for the interval τ_{est}. For the given cases, namely, IM, EM-AC and EM-OC, a suitable sensing time that results in a maximum throughput $R_s(\tau_{est} = 5\,\text{ms}, \tilde{\tau}_{sen})$ is determined. Hence, a performance degradation is depicted in terms of the achievable throughput, cf. Fig. 6. For $\kappa = 0.05$, it is observed that the outage constraint

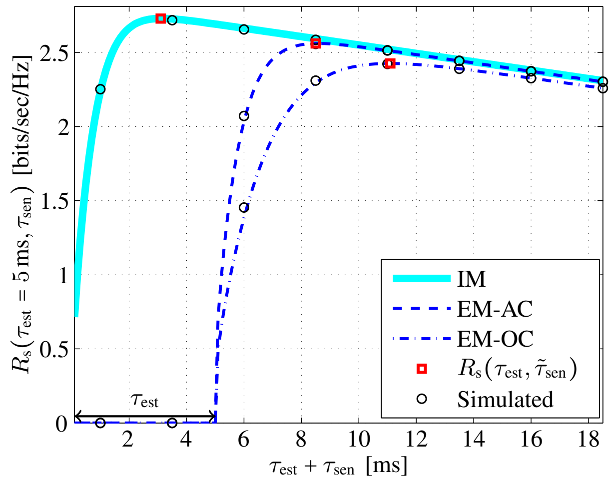

Fig. 6. Sensing-throughput tradeoff for the ideal and estimation models with $\gamma_{p,1} = -10$ dB, $\tau_{est} = 5$ ms and $\kappa = 0.05$.

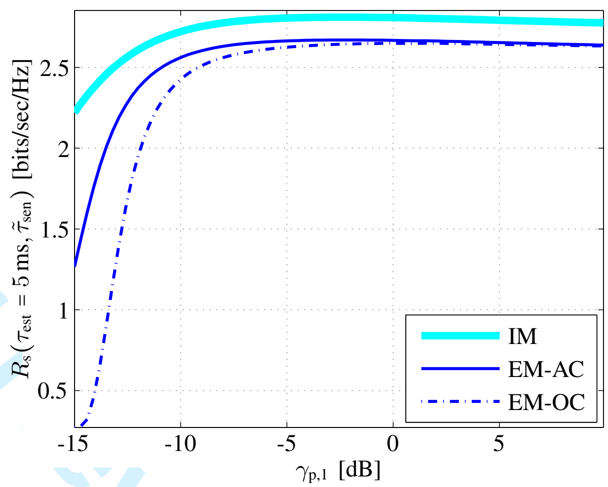

Fig. 7. Achievable throughput versus $\gamma_{p,1}$ with $\tau_{est} = 5$ ms.

is more sensitive to the performance loss in comparison to average constraint. It is clear that the analysis illustrated Fig. 6 is obtained for a certain choice of system parameters, particularly $\gamma_{p,1} = -10$ dB, $\tau_{est} = 5$ ms and $\kappa = 0.05$. To acquire more insights, we consider the effect of variation of these parameters on the performance of IS, subsequently.

Hereafter, for the analysis, we consider the theoretical expressions and choose to operate at suitable sensing time. Next, we determine the variations of the achievable throughput against the received signal to noise ratio $\gamma_{p,1}$ at the ST with $\tau_{est} = 5$ ms, cf. Fig. 7. For $\gamma_{p,1} < -5$ dB, the estimation model incurs a significant performance loss. This clearly reveals that the ideal model overestimates the performance of IS. Hence, it is perceived that despite loss in performance, the estimation model is capable of precluding interference at the PR, hence, assuring reliability to the system.

Upon maximizing the secondary throughput, it is interesting to analyze the variation of achievable throughput with the estimation time. Corresponding to the estimation model, Fig. 8 illustrates a tradeoff among the estimation time, the sensing time and the throughput, cf. Corollary 1. This can be explained

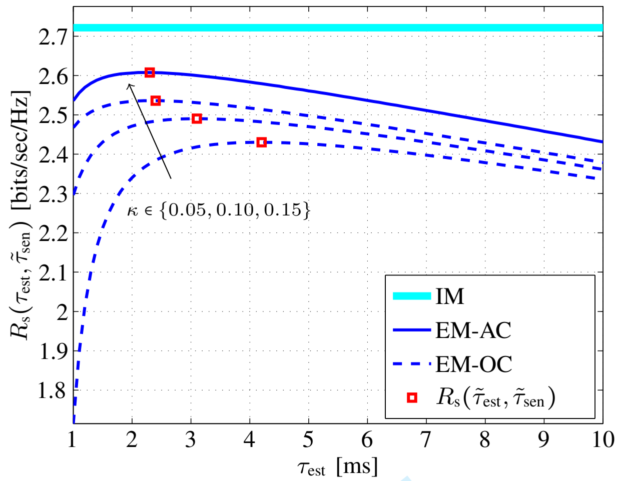

Fig. 8. Estimation-throughput tradeoff for the average and outage constraints with $\gamma_{p,1} = -10\,$dB, where the throughput is maximized over the sensing time, $R_s(\tau_{est}, \tilde{\tau}_{sen})$. Estimation-throughput tradeoff is utilized to determine a suitable estimation time $\tilde{\tau}_{est}$ that maximizes the throughput, $R_s(\tilde{\tau}_{est}, \tilde{\tau}_{sen})$.

from the fact that low values of estimation time result in large variation in P_d. To counteract and satisfy the average and outage constraints, the corresponding thresholds shift to a lower value. This causes an increase in P_{fa}, thereby increasing the sensing-throughput curvature. As a result, the suitable sensing time is obtained at a higher value. However, beyond a certain value ($\tilde{\tau}_{est}$), a further increase in estimation time slightly contributes to performance improvement and largely consumes the time resources. As a consequence to the estimation-sensing-throughput tradeoff, we determine the suitable estimation time that yields an achievable throughput $R_s(\tilde{\tau}_{est}, \tilde{\tau}_{sen})$. Besides that, we consider the variation of achievable throughput for different values of the outage constraint, cf. Fig. 8. It is observed that for the selected choice of κ, the outage constraint is severe as compared to the average constraint, hence, results in a lower throughput. Thus, depending on the nature of policy (aggressive or conservative) followed by the regulatory bodies towards interference at the primary system, it is possible to define κ accordingly during the system design.

To procure further insights, we investigate the variations of expected P_d and P_{fa} with the estimation time. From Fig. 9a, it is observed that the expected P_d corresponding to the outage constraint is strictly above the desired level $\bar{P}_d$ for all values of estimation time, however, for lower values of estimation time, this margin reduces. This is based on the fact that lower estimation time shifts the probability mass of P_d, to a lower value, cf. Fig. 3a. Besides that, based on the previous discussion, it was analyzed that P_{fa} accounts for a large contribution to the throughput. According to Fig. 9b, P_{fa} witnesses a large improvement in performance in the regime $\tau_{est} \leq 3\,$ms, however, saturates in the regime $\tau_{est} \geq 3\,$ms, thus, provides further justification to the variation of $R_s(\tau_{est}, \tilde{\tau}_{sen})$ against τ_{est} characterized as estimation-sensing-throughput tradeoff depicted in Fig. 8.

VI. Conclusion

In this paper, we have investigated the performance of cognitive radio as an interweave system from a deployment perspective. It has been argued that the knowledge of the interacting channels is a key aspect that enables the performance characterization of the interweave system in terms of sensing-throughput tradeoff. In this regard, a novel model that facilitates channel estimation and captures the effect of estimation in the system model has been proposed. As a major outcome of the analysis, it has been justified that the existing model, illustrating an ideal scenario, overestimates the performance of the interweave system, hence, less suitable for deployment. Moreover, it has been indicated that the variation induced in the system, specially in the detection probability may severely degrade the performance of the primary system. To overcome this situation, average and outage constraints as primary user constraints have been employed. As a consequence, for the proposed estimation model, novel expressions for sensing-throughput tradeoff based on the mentioned constraints have been established. More importantly, by analyzing the estimation-sensing-throughput tradeoff, suitable estimation time and sensing time that maximizes the secondary throughput have been determined. In our future work, we plan to extend the proposed analysis for the hybrid cognitive radio system that combines the advantages of interweave and underlay techniques.

References

[1] A. Kaushik, S. K. Sharma, S. Chatzinotas, B. Ottersten, and F. K. Jondral, "Sensing-Throughput Tradeoff for Cognitive Radio Systems with Unknown Received Power," in *10th International Conference on Cognitive Radio Oriented Wireless Networks and Communications (CROWNCOM)*, April 2015.

[2] J. Andrews, S. Buzzi, W. Choi, S. Hanly, A. Lozano, A. Soong, and J. Zhang, "What Will 5G Be?" *IEEE Journal on Selected Areas in Communications*, vol. 32, no. 6, pp. 1065–1082, June 2014.

[3] T. Rappaport, S. Sun, R. Mayzus, H. Zhao, Y. Azar, K. Wang, G. Wong, J. Schulz, M. Samimi, and F. Gutierrez, "Millimeter Wave Mobile Communications for 5G Cellular: It Will Work!" *IEEE Access*, vol. 1, pp. 335–349, 2013.

[4] J. Mitola and G. Q. Jr. Maguire, "Cognitive radio: making software radios more personal," *IEEE Personal Communications*, vol. 6, no. 4, pp. 13–18, August 1999.

[5] A. Goldsmith, S. Jafar, I. Maric, and S. Srinivasa, "Breaking Spectrum Gridlock With Cognitive Radios: An Information Theoretic Perspective," *Proceedings of the IEEE*, vol. 97, no. 5, pp. 894–914, May 2009.

[6] S. Sharma, T. Bogale, S. Chatzinotas, B. Ottersten, L. Le, and X. Wang, "Cognitive Radio Techniques under Practical Imperfections: A Survey," *IEEE Communications Surveys Tutorials*, vol. PP, no. 99, pp. 1–1, 2015.

[7] E. Axell, G. Leus, E. Larsson, and H. Poor, "Spectrum Sensing for Cognitive Radio : State-of-the-Art and Recent Advances," *IEEE Signal Processing Magazine*, vol. 29, no. 3, pp. 101–116, May 2012.

[8] H. Urkowitz, "Energy detection of unknown deterministic signals," *Proceedings of the IEEE*, vol. 55, no. 4, pp. 523 – 531, april 1967.

[9] V. Kostylev, "Energy detection of a signal with random amplitude," in *IEEE ICC*, vol. 3, 2002, pp. 1606–1610.

[10] F. Digham, M.-S. Alouini, and M. K. Simon, "On the energy detection of unknown signals over fading channels," in *IEEE ICC*, vol. 5, May 2003, pp. 3575–3579.

[11] S. Herath, N. Rajatheva, and C. Tellambura, "Unified Approach for Energy Detection of Unknown Deterministic Signal in Cognitive Radio Over Fading Channels," in *IEEE ICC Workshops*, June 2009, pp. 1–5.

[12] A. Mariani, A. Giorgetti, and M. Chiani, "Energy detector design for cognitive radio applications," in *2010 International Waveform Diversity and Design Conference (WDD)*, Aug 2010, pp. 053–057.

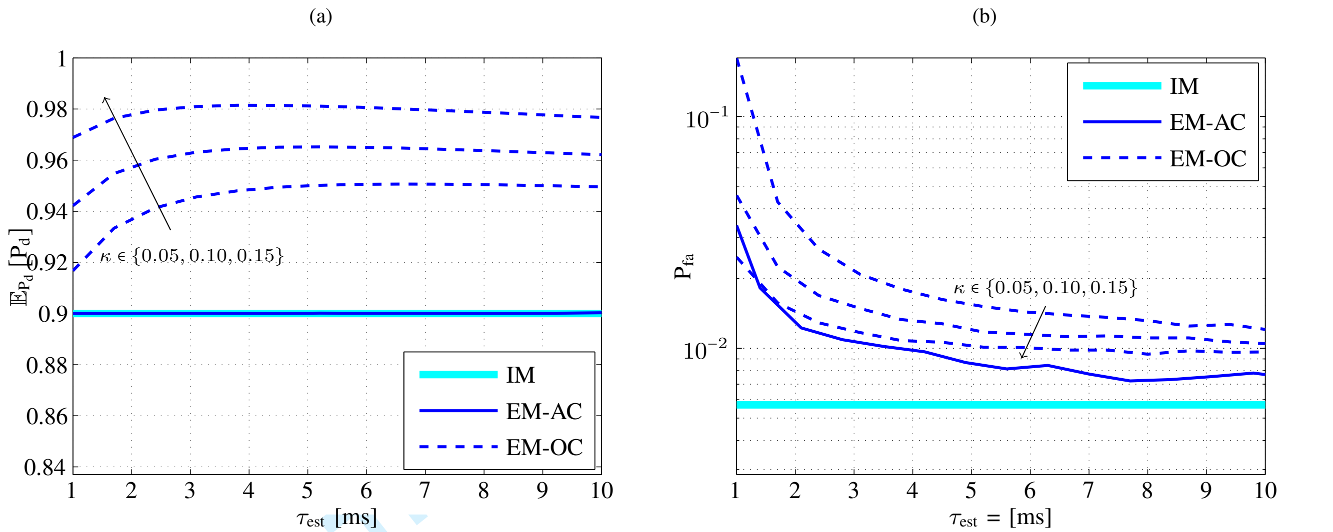

Fig. 9. Variation of $\mathbb{E}_{\mathrm{P_d}}[\mathrm{P_d}]$ and $\mathrm{P_{fa}}$ versus the τ_{est}, where the secondary throughput is maximized over the sensing time, $R_{\mathrm{s}}(\tau_{\mathrm{est}}, \tilde{\tau}_{\mathrm{sen}})$. (a) Expected $\mathrm{P_d}$ versus τ_{est}, (b) $\mathrm{P_{fa}}$ versus τ_{est}.

[13] E. Peh and Y.-C. Liang, "Optimization for cooperative sensing in cognitive radio networks," in *IEEE Wireless Communications and Networking Conference (WCNC)*, March 2007, pp. 27–32.

[14] Y.-C. Liang, Y. Zeng, E. Peh, and A. T. Hoang, "Sensing-Throughput Tradeoff for Cognitive Radio Networks," *IEEE Transactions on Wireless Communications*, vol. 7, no. 4, pp. 1326–1337, April 2008.

[15] S. Sharma, S. Chatzinotas, and B. Ottersten, "A hybrid cognitive transceiver architecture: Sensing-throughput tradeoff," in *CROWNCOM*, Jun. 2014.

[16] H. Pradhan, S. Kalamkar, and A. Banerjee, "Sensing-Throughput Tradeoff in Cognitive Radio With Random Arrivals and Departures of Multiple Primary Users," *IEEE Communications Letters*, vol. 19, no. 3, pp. 415–418, March 2015.

[17] M. K. Simon and M. S. Alouini, *Digital Communication over Fading Channels: A Unified Approach to Performance Analysis*, 1st ed. New York: Wiley, 2000.

[18] A. Kaushik, M. R. Raza, and F. K. Jondral, "On the Deployment of Cognitive Relay as Underlay Systems," in *CROWNCOM*, Jun. 2014.

[19] M. Cardenas-Juarez and M. Ghogho, "Spectrum Sensing and Throughput Trade-off in Cognitive Radio under Outage Constraints over Nakagami Fading," *IEEE Communications Letters*, vol. 15, no. 10, pp. 1110–1113, October 2011.

[20] Y. Sharkasi, M. Ghogho, and D. McLernon, "Sensing-throughput tradeoff for OFDM-based cognitive radio under outage constraints," in *ISWCS*, Aug 2012, pp. 66–70.

[21] R. Tandra and A. Sahai, "SNR Walls for Signal Detection," *IEEE Journal of Selected Topics in Signal Processing*, vol. 2, no. 1, pp. 4–17, Feb 2008.

[22] M. Gans, "The Effect of Gaussian Error in Maximal Ratio Combiners," *IEEE Transactions on Communication Technology*, vol. 19, no. 4, pp. 492–500, August 1971.

[23] W. Gifford, M. Win, and M. Chiani, "Diversity with practical channel estimation," *IEEE Transactions on Wireless Communications*, vol. 4, no. 4, pp. 1935–1947, July 2005.

[24] ——, "Antenna subset diversity with non-ideal channel estimation," *IEEE Transactions on Wireless Communications*, vol. 7, no. 5, pp. 1527–1539, May 2008.

[25] R. Annavajjala and L. Milstein, "Performance analysis of linear diversity-combining schemes on Rayleigh fading channels with binary signaling and Gaussian weighting errors," *IEEE Transactions on Wireless Communications*, vol. 4, no. 5, pp. 2267–2278, Sept 2005.

[26] H. Suraweera, P. Smith, and M. Shafi, "Capacity limits and performance analysis of cognitive radio with imperfect channel knowledge," *IEEE Transactions on Vehicular Technology*, vol. 59, no. 4, pp. 1811–1822, May 2010.

[27] H. Kim, H. Wang, S. Lim, and D. Hong, "On the Impact of Outdated Channel Information on the Capacity of Secondary User in Spectrum Sharing Environments," *IEEE Transactions on Wireless Communications*, vol. 11, no. 1, pp. 284–295, January 2012.

[28] A. Kaushik, S. K. Sharma, S. Chatzinotas, B. Ottersten, and F. K. Jondral, "Estimation-Throughput Tradeoff for Underlay Cognitive Radio Systems," *IEEE ICC 2015 - Cognitive Radio and Networks Symposium (ICC'15 (12) CRN)*, Jun. 2015.

[29] A. Kaushik, M. Mueller, and F. K. Jondral, "Cognitive Relay: Detecting Spectrum Holes in a Dynamic Scenario," in *ISWCS*, Apr. 2013, pp. 1–2.

[30] T. Wang, Y. Chen, E. Hines, and B. Zhao, "Analysis of effect of primary user traffic on spectrum sensing performance," in *Fourth International Conference on Communications and Networking in China*, Aug 2009, pp. 1–5.

[31] L. Tang, Y. Chen, E. Hines, and M.-S. Alouini, "Effect of Primary User Traffic on Sensing-Throughput Tradeoff for Cognitive Radios," *IEEE Transactions on Wireless Communications*, vol. 10, no. 4, pp. 1063–1068, April 2011.

[32] B. Zhao, Y. Chen, C. He, and L. Jiang, "Performance analysis of spectrum sensing with multiple primary users," *IEEE Transactions on Vehicular Technology*, vol. 61, no. 2, pp. 914–918, Feb 2012.

[33] S. Kay, *Fundamentals of Statistical Signal Processing: Detection theory*, ser. Prentice Hall Signal Processing Series. Prentice-Hall PTR, 1998.

[34] I. S. Gradshteyn and I. M. Ryzhik, *Table of Integrals, Series, and Products*, 6th ed. San Diego, CA: Academic Press., 2000.

[35] M. Abramowitz and I. A. Stegun, *Handbook of Mathematical Functions with Formulas, Graphs, and Mathematical Tables*, ninth Dover printing, tenth GPO printing ed. New York: Dover, 1964.

[36] F. W. J. Olver, D. W. Lozier, R. F. Boisvert, and C. W. Clark, Eds., *NIST Handbook of Mathematical Functions*. New York, NY: Cambridge University Press, 2010.